DOI:
10.1172/jci.insight.130540

Document Version
Peer reviewed version

JCI insight

BCG revaccination boosts adaptive polyfunctional Th1/Th17 and innate effectors in IGRA$^+$ and IGRA$^-$ Indian adults

Srabanti Rakshit, … , M. Juliana McElrath, Annapurna Vyakarnam

JCI Insight. 2019. https://doi.org/10.1172/jci.insight.130540.

Clinical Medicine | In-Press Preview | Immunology | Infectious disease

Graphical abstract

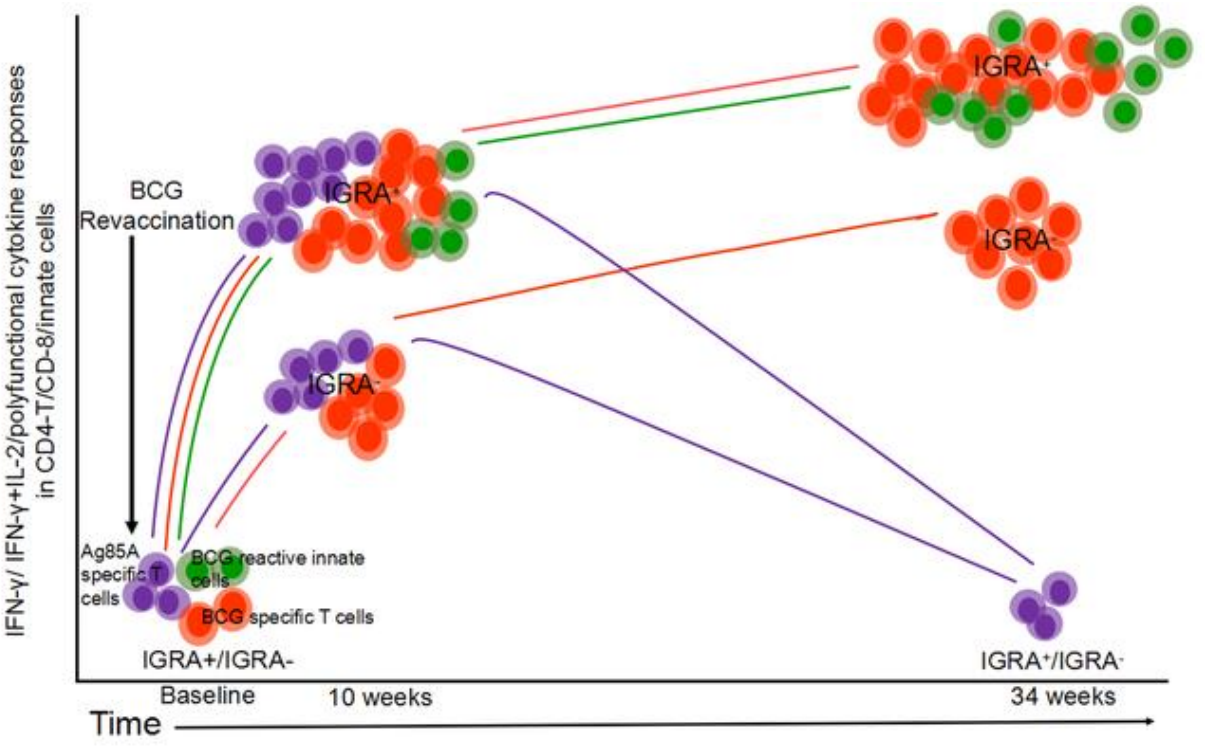

Find the latest version:

http://jci.me/130540/pdf

BCG revaccination boosts adaptive polyfunctional Th1/Th17 and innate effectors in IGRA$^+$ and IGRA$^-$ Indian adults

Srabanti Rakshit[1#], Asma Ahmed[1#], Vasista Adiga[1], Bharath K. Sundararaj[1], Pravat Nalini Sahoo[1], John Kenneth[2]; George D' Souza[2]; Wesley Bonam[3], Christina Johnson[3], Kees LMC Franken[4], Tom H.M. Ottenhoff[4], Greg Finak[5], Raphael Gottardo[5], Kenneth D. Stuart[6], Stephen C. De Rosa[5], M. Juliana McElrath[5,7**], Annapurna Vyakarnam[1,8**]

[1]Laboratory of Immunology of HIV-TB Co-infection, Centre for Infectious Disease Research, Indian Institute of Science, Bangalore, India.

[2]Department of Infectious Diseases & Department of Pulmonary Medicine, St John's Research Institute, Bangalore, India.

[3]Arogyavaram Medical Centre, Madanapalle, India.

[4]Department of Infectious Diseases, Leiden University Medical Center, Leiden, Netherlands

[5]Vaccine and Infectious Disease Division, Fred Hutchinson Cancer Research Center, Seattle, WA, USA.

[6]Seattle Children's Research Institute, Seattle, WA, United States of America

[7]Department of Medicine, University of Washington School of Medicine, Seattle, WA, USA.

[8]Peter Gorer Department of Immunobiology, School of Immunology and Microbial Sciences, Faculty of Life Sciences & Medicine, Guy's Hospital, King's College London, London SE1 9RT, UK.

[#]S.R. and A.A contributed equally

** Equal Joint Senior Authors

***Correspondence to:**

Dr. M. Juliana McElrath; Vaccine and Infectious Disease Division, Fred Hutchinson Cancer Research Center, Seattle, WA, United States of America.

jmcelrat@fredhutch.org

And

Dr. Annapurna Vyakarnam; Centre for Infectious Disease Research Indian Institute of Science; Bangalore 560012 and Department of Immunobiology, School of Immunology & Microbial Sciences, King's College London

Tel: 0091-80-2360-4348 (land line, India)/0091-9945385960 (mobile, India)

E-mail: anna.vyakarnam@kcl.ac.uk, annapurna@iisc.ac.in

ABSTRACT

Background: Bacille Calmette-Guérin (BCG) vaccine is protective in children but its efficacy wanes with age. Consequently, determining if BCG revaccination augments anti-TB immunity in young adults in TB endemic regions is vital.

Methods: 200 healthy adults, BCG vaccinated at birth were tested for their IGRA status. Of these, 28 $IGRA^+$ and 30 $IGRA^-$ were BCG revaccinated and 24 $IGRA^+$ and 23 $IGRA^-$ subjects served as unvaccinated controls. T and innate cell responses to mycobacterial antigens were analysed by 14-colour flow cytometry over 34 weeks.

Results: IFN-γ and/or IL-2 Ag85A and BCG-specific $CD4^+$ and $CD8^+$ T-cell responses were boosted by revacciantion at 4 and 34 weeks respectively and were >2-fold higher in $IGRA^+$ compared to $IGRA^-$ vaccinees. Polyfunctional Ag85A, BCG and Mtb latency Ag (LTAg)-specific $CD4^+$ T-cells expressing up to 8 cytokines were also significantly enhanced in both $IGRA^+$ and $IGRA^-$ vaccinees relative to unvaccinated controls, most markedly in $IGRA^+$ vaccinees. A focussed analysis of Th17 responses revealed expansion of Ag85A, BCG and LTAg-specific total IL-$17A^+$IL-$17F^+$IL-22^+ and IL-10^+ $CD4^+$ T-cell effectors in both $IGRA^+$ and $IGRA^-$ subjects. Also, innate IFN-γ^+ NK/γδ/NKT responses were higher in both $IGRA^+$ and $IGRA^-$ vaccinees compared to controls. This is the first evidence that BCG revaccination significantly boosts anti-mycobacterial Th1/Th17 responses in $IGRA^+$ and $IGRA^-$ subjects.

Summary: These data show that BCG revaccination is immunogenic in $IGRA^-$ and $IGRA^+$ subjects implying that Mtb pre-infection in $IGRA^+$ subjects does not impact immunogenicity. This has implications for public health and vaccine development strategies.

Funding: This work was funded principally by DBT-NIH (BT/MB/Indo-US/HIPC/2013).

INTRODUCTION

Tuberculosis (TB) is the leading cause of death from a single infectious agent, *Mycobacterium tuberculosis* (Mtb). An estimated 10.4 million new TB cases occurred in 2017 (1). Almost a quarter of the world's population in Asia and Africa is estimated to have latent Mtb infection (1, 2). These individuals generally develop active TB within five years of initial infection, while approximately 5-10% of those infected are at a higher risk of progressing towards disease during their lifetimes (3). BCG, a live attenuated strain of *Mycobacterium bovis,* first introduced in 1921, is the only clinically approved TB vaccine (4). Although BCG administered at birth significantly reduces the incidence of severe miliary and meningeal TB in infants and children, it is less effective against pulmonary TB in adults, the most common form of TB disease and the major source of transmission worldwide (5-8). Meta-analysis of 14 prospective BCG efficacy studies involving 3855 participants revealed an estimated protective efficacy of 19% against Mtb infection based on interferon gamma (IFN-γ) release assay (IGRA) positivity and 58% against TB disease (9). Clearly, a more effective TB vaccine strategy is needed worldwide, and efforts to understand protective immunity against Mtb infection are a major global research priority. Here, we present a study designed to investigate the effects of BCG revaccination in boosting Mtb immunity in South Indian young adults, who are highly vulnerable to TB disease as their immunity to Mtb is likely waning since vaccination at birth.

Many factors can account for the variable efficacy of BCG in different countries, but a consistent theme is that efficacy is suboptimal and protection wanes as children reach adolescence. Thus, the protective efficacy of BCG administered at birth rarely persists beyond 15-20 years in TB endemic regions; is highly variable in adults (6, 8) and differs considerably with geographical location and prior sensitization to Mtb or

even other environmental and non-tuberculous mycobacteria (NTM) (10-12). Evidence from other studies shows that BCG and NTM responses can influence each other. BCG vaccination can offer protection against NTM infection in children (13, 14). BCG administration and *M. tuberculosis* infection in mice and human induces NTM cross-reactive T-cells (15). A 15-year follow-up of a randomized controlled BCG trial in South India, average protection was 32% (95% CI: 3–52%) among people who were initially non-responsive to NTMs detected by a Tuberculin Skin Test (TST); by contrast, no significant protection was observed in vaccine recipients previously exposed to NTMs (16). On the other hand, there is also evidence to suggest that prior exposure to NTM can affect BCG vaccine efficacy and the results of PPD skin test (17). Some have postulated that the lack of sustained protection after BCG vaccination may relate to the failure to establish a long-term central memory response (18). Furthermore, a reduced protective effect of BCG may occur with co-infections, especially HIV-1 infection (6, 7, 19), a known major predisposing factor for TB incidence (20-22).

Recent efforts have focused on developing improved vaccines to prevent Mtb infection, since such a vaccine could have a high population-level impact for TB control and tailored pre-existing immunity may be more effective during acute infection than after persistent chronic infection (23). Current approaches under evaluation in animal models and some in humans include: 1) recombinant live attenuated vaccines with improved efficacy over BCG, such as new mycobacterial vaccine designs, as well as CMV and chimp adenovirus vectors containing Mtb antigens, 2) boosting BCG with homologous BCG or subunit vaccines such as H4:IC31 and 3) delivery of TB vaccines by aerosolization rather than systemically (24-27). Revaccination with BCG in adolescence has been in routine practice in many countries throughout the world with variable benefit (28). Moreover, BCG

132 revaccination in diverse age groups and regional TB incidence has yielded
133 inconsistent levels of protection against TB disease (29-42).

134

135 There is renewed interest in BCG revaccination of young adults, especially in
136 countries with high TB burden (43-44), based on recent positive results from the
137 Aeras C-040-404 randomized, placebo-controlled, prevention of infection TB vaccine
138 study (45). This study was conducted in the Western Cape Province of South Africa
139 among 990 HIV-negative, healthy adolescents BCG vaccinated at birth. Mtb-
140 uninfected subjects were randomized to receive either placebo, H4:IC31, or BCG
141 revaccination. When compared to placebo, neither vaccine achieved statistical
142 significance in preventing an initial QFT-GIT conversion. However, analysis of the
143 secondary efficacy endpoint indicated that BCG revaccination reduced sustained Mtb
144 infection in young adolescents by 45.4% and H4:IC31 reduced sustained Mtb
145 infection by 30.5% (45). A follow up efficacy trial is planned to confirm these findings
146 and to examine potential biomarkers of protective immunity.

147

148 Few studies have reported detailed analysis of the immune profile alterations
149 following BCG revaccination in humans, and among these, populations evaluated
150 have varied by age group and status of Mtb infection. Revaccination of infants
151 induced a significant increase in IFN-γ and IL-10 concentrations in three-day whole
152 blood culture supernatants to PPD stimulation (46, 47). Others have reported that
153 BCG revaccination of TST-positive subjects on INH treatment elicited long-lived
154 memory NK and NKT-like cells besides transiently boosting BCG-specific Th1
155 cytokines in $CD4^+$, $CD8^+$ and T-cell receptor (TCR) γδ cells using an intracellular
156 cytokine staining (ICS) assay (48). In an extensive immune profiling study, we
157 recently reported a key distinguishing feature of subjects with latent TB infection (not

158 on INH treatment) to be the presence of circulating Mtb-specific central memory
159 polyfunctional $CD4^+$ T-cells, that co-expressed IL-17A/IL-17F/IL-22 with IL-10; this
160 specific Th17 subset was either lacking or significantly reduced in the
161 bronchoalveolar lavage of subjects with pulmonary disease or in the blood of
162 subjects with extrapulmonary TB (49). By contrast, subjects with either pulmonary or
163 extrapulmonary TB had expanded frequencies of pro-inflammatory Th17 cells that
164 co-expressed IL-17A/IL-17F/IL-22 with IFN-γ (49). These data from our laboratory on
165 a potential role for Mtb-specific $IL\text{-}17^+$ and $IL\text{-}10^+$ cells in anti-TB immunity has been
166 extended in a recent publication using a macaque in vivo TB challenge model, which
167 highlighted the key cells associated with protection against live bacterial challenge
168 following BCG vaccination to be Mtb-specific $CD4^+$ T-cells that expressed IL-17 and
169 other IL-10 producing immune cells (50). Therefore, a major aim of our current study
170 was to determine if BCG revaccination can boost circulating frequencies of Mtb-
171 specific Th17 $CD4^+$ T-cells in both $IGRA^+$ and $IGRA^-$ young adults, a highly
172 vulnerable population, living in an HIV endemic area of South India.

173

174 Detailed immune profiling of subjects following BCG revaccination, has not been
175 reported from India. We present novel data to show that BCG revaccination of young
176 adults in India can enhance a Mtb-specific $CD4^+$ T-cell immune signature potentially
177 associated with controlled TB infection.

178

RESULTS

Mtb antigen-specific CD4⁺ T-cells are preserved in young adults receiving BCG at birth

Two hundred volunteers who were HIV-ve, TB-ve, Hep B Ab-ve and BCG vaccinated at birth, living in Madanapalle, India, were recruited (Figure 1A). Volunteers were divided into four groups based on both screening for IGRA status and then randomisation to receive BCG revaccination at T0 (Figure 1, A and B). All volunteers subsequently received three doses of hepatitis B virus surface antigen vaccine at weeks 4 (T2), 10 (T4) and 30 (Figure 1, A and B) (see materials and methods). The median age of the study population was 20 years (range, 18-28 years) and 58.75% were female (Table 1, Supplemental File 1). The approximate male:female ratio in different clinical groups was: Groups 1 43:57, Group 2: 39:61, Group 3 - 61:39 and Group 4 -22:78. The median IGRA levels in Groups 1 and 3 were similar (median for Group 1 - 3.6; for Group 3 – 2; range 0.46-10). The median IGRA values for $IGRA^-$ subjects (Groups 2 and 4) were ≤ 0.1 (range 0 – 0.3) (Table 1, Supplemental File 1).

Multiparameter flow cytometry was performed on whole blood to assess the presence of T-cells recognizing Mtb antigens prior to revaccination (Ag85A, TB10.4, BCG), which would reflect baseline responses maintained either by BCG vaccination at birth and/or prior exposure to cross-reactive NTM. Representative whole blood flow cytometry plots depicting the stepwise gating strategy to identify functional subsets are shown in Supplemental Figure 1. Cross-sectional analysis of baseline $CD4^+$ T-cell responses measured as frequencies of IFN-γ and/or IL-2 expressing cells in $IGRA^+$ vs. $IGRA^-$ donors revealed that recall responses to Mtb antigens TB10.4 and Ag85A, and BCG (used as antigen for *in vitro* stimulation) were well preserved in both groups, with high basal responses particularly to BCG antigens (Figure 2). As expected, $IGRA^+$ subjects had significantly higher baseline $CD4^+$ T-cell

responses to epitopes in BCG and TB10.4 compared to IGRA$^-$ subjects recruited to the study (Figure 2). Baseline antigen-specific CD8$^+$ T-cell frequencies were generally lower than the CD4$^+$ T-cell frequencies, and notably the BCG-specific CD8$^+$ T-cell responses were greater than the responses to Ag85A and TB10.4 (Figure 2). No significant differences were observed between the median IGRA$^+$ and IGRA$^-$ CD8$^+$ T-cell recall responses at baseline (Figure 2). These data provide clear evidence of baseline CD4$^+$ T-cell responses to Ag85A and TB10.4 peptides in IGRA$^+$ and IGRA$^-$ subjects and to epitopes presented by BCG with the magnitude of this baseline response varying significantly between donors in a group. These data indicate preservation of memory CD4$^+$ T-cells recognizing BCG and *Mtb* antigens in both IGRA$^+$ and IGRA$^-$ volunteers recruited to this study, reflecting responses either induced by BCG vaccination at birth or by exposure to environmental cross-reactive mycobacteria.

Longitudinal analysis reveals BCG revaccination significantly enhances Ag85A- and BCG-specific CD4$^+$ and CD8$^+$ T-cell responses

We next determined whether BCG revaccination could increase Mtb-specific CD4$^+$ and CD8$^+$ T-cell responses in whole blood of IGRA$^+$ and IGRA$^-$ young adults above baseline responses in a longitudinal study with representative gating shown in Supplemental Figure 1. We demonstrate significant enhancement post vaccination, in frequencies of Ag85A (Figure 3A) and BCG (Figure 3E) specific CD4$^+$ T-cells expressing IFN-γ and/or IL-2. The peak median fold increase over baseline was 2.3 fold for Ag85A (at T2) and 5.7-fold for BCG (at T5) in Group 1 IGRA$^+$ subjects (Figure 3, B and F). Similar enhancement was also noted for Ag85A (Figure 3B) but not BCG (Figure 3F) specific CD4$^+$ T-cell frequencies in Group 2 IGRA$^-$ vaccinees, possibly due to baseline responses in the IGRA$^-$ subjects being lower than the IGRA$^+$ subjects (see Figure 2). By comparison, these responses did not significantly differ over time in non-vaccinated Group 3 and 4 control subjects (Figure 3, B and F). Evidence of an

232 enhanced $CD4^+$ T-cell response in vaccinees was maintained in a cross-sectional
233 analysis of this data, despite significant intra-group variation. Thus, higher Ag85A
234 (Figure 3C) and BCG (Figure 3G) specific IFN-γ^+ and/or IL-2^+ $CD4^+$ T-cell
235 frequencies were noted in Group 1 compared to Group 3 subjects, with Ag85A
236 responses peaking at T2 (Figure 3C) and BCG responses at T5 (Figure 3G).

237 BCG revaccination substantially enhanced Ag85A (Figure 4A) and BCG (Figure 4E)
238 specific IFN-γ^+ and/or IL-2^+ $CD8^+$ T-cell frequencies. In Group 1 $IGRA^+$ vaccinees,
239 median $CD8^+$ T-cell responses were enhanced above baseline (T0) by 15.1 fold for
240 Ag85A at T2 (Figure 4B) and 14.4 fold for BCG at T5 (Figure 4F). However, in Group
241 2 $IGRA^-$ vaccinees, only Ag85A but not BCG specific $CD8^+$ T-cell responses were
242 boosted (Figure 4, B and F). This enhancement was not observed in unvaccinated
243 Group 3 and Group 4 control subjects (Figure 4, B and F). Cross-sectional analysis
244 of this data showed higher $CD8^+$ T-cell responses to Ag85A at T2 but not to BCG in
245 Group 1 'vs' Group 3 (Figure 4, C and G).

246 The memory composition of vaccine-induced T-cells was analysed using CD45RA
247 and CD27 markers. The baseline IFN-γ and/or IL-2 expressing $CD4^+$ T-cells specific
248 for Ag85A and BCG comprised a mixture of naïve (N), central memory (CM), effector
249 memory (EM) and terminally differentiated effector memory expressing CD45RA
250 (TD) cells (Figure 3, D and H). BCG revaccination expanded Ag85A-specific $CD4^+$
251 EM T-cells in Group 1 $IGRA^+$ subjects but not Group 2 $IGRA^-$ subjects at T2 (4
252 weeks) relative to T0 (Figure 3D); in contrast, there was no significant change in
253 memory subset composition in BCG-specific cells (Figure 3H). In addition, there were
254 no significant longitudinal changes in subset composition in the $CD8^+$ T-cell
255 compartment (Figure 4, D and H).

256 The Mtb-specific vaccine induced T-cell response was probed further by analysing
257 $CD4^+$ and $CD8^+$ T-cell frequencies to another immunodominant antigen, namely TB

10.4, which is a part of the well-recognised *esat*-6 gene family (51) using a pool of overlapping peptides. In contrast to Ag85A and BCG-specific responses, TB10.4 responses were not significantly induced in both IGRA$^+$ and IGRA$^-$ vaccinees (see Supplemental Figure 2), demonstrating selectivity in the enhancement of Mtb-specific responses by revaccination.

Finally, a comparison of immunostaining of matched whole blood and PBMC samples in ten subjects showed significant correlation (Figure 5A). Representative PBMC flow cytometry plots depicting gating strategy is shown in Supplemental Figure 3. Ag85A and BCG-specific IFN-γ$^+$ and/or IL-2$^+$ CD4$^+$ T-cell frequencies show significantly higher frequencies over baseline T0 responses with Ag85A at T2 and BCG at T5 in Group 1 IGRA$^+$ in whole blood and PBMC (Figure 5B). Taken together, these data provide strong evidence of the capacity of BCG revaccination to significantly boost IFN-γ$^+$ and/or IL-2$^+$ CD4$^+$ and CD8$^+$ T-cell responses in IGRA$^+$ subjects over and above the inherently variable baseline responses. Also, the data shows that BCG revaccination induced a transient increase of Ag85A responses in Group 2 IGRA$^-$ participants, but not to BCG.

Longitudinal analysis reveals BCG revaccination to significantly enhance Ag85A- and BCG-specific CD4$^+$ and CD8$^+$ T-cell polyfunctional response in both IGRA$^+$ and IGRA$^-$ subjects

To examine co-expression of effector cytokines, we used COMPASS, as in our previous study (49) to enumerate antigen-specific polyfunctional responses of total CD4$^+$ and CD8$^+$ T-cells, in whole blood samples by analysing all 64 possible combinations of IFN-γ, IL-2, TNF-α, IL-17A and MIP-1β. Polyfunctional responses to Ag85A and BCG stimulation were determined over time and summarized through the COMPASS polyfunctionality score (PFS) (Figure 6). Differences in PFS between groups were estimated through a linear model fit to the PFS for each antigen (see

Methods). After multiple testing adjustments, significant increase in PFS scores compared to baseline were observed in Group 1 IGRA$^+$ and Group 2 IGRA$^-$ CD4$^+$ T-cell responses to BCG epitopes at T5 and in Group 2 Ag85A-specific CD4$^+$ T-cells at T2. Polyfunctional CD8$^+$ T-cell responses were significantly enhanced over baseline in Group 1 in response to both Ag85A at T2 and BCG epitopes at T5, and in Group 2 in response to Ag85A at T2. However, no increase in CD4$^+$ and CD8$^+$ T-cell PFS was noted in subjects from unvaccinated controls in Groups 3 (IGRA$^+$) and 4 (IGRA$^-$), relative to baseline responses at T0. The CD4$^+$ T-cell polyfunctionality response to BCG was more prominent than the CD8$^+$ T-cell response, whereas the Ag85A-specific CD8$^+$ polyfunctional response was the dominant one compared to its CD4$^+$ response as reflected in the p-values between T0 'vs' T2 for Ag85A and T0 'vs' T5 for BCG in both Group 1 and 2 (Figure 6).

Heatmaps were constructed to identify the specific combinations of immune subsets that were expanded by BCG revaccination in Groups 1 and 2. Data from all subjects in the four clinical groups were analyzed for CD4$^+$ (Figure 7, upper panel) and CD8$^+$ (Figure 7, lower panel) polyfunctional T-cell responses at baseline and at T2 and T5 post-BCG vaccination following Ag85A and BCG stimulation respectively. The Ag85A-specific CD4$^+$ T-cell response was more marked in IGRA$^+$ Group 1 vaccinees with enhanced expression of 1$^+$ (IFN-γ, MIP-1β), 2$^+$ (TNF-α/MIP-1β, IFN-γ/MIP-1β) and 3$^+$ (IFN-γ/TNF-α/MIP-1β) subsets compared to baseline or Group 3 unvaccinated controls. The data also highlight the CD4$^+$ T-cell responses induced by BCG antigens were more polyfunctional compared to those induced by Ag85A, with higher frequencies of 3$^+$ and 4$^+$ cells producing different combinations of IFN-γ, IL-2, IL-17, TNF-α and MIP-1β in addition to 1$^+$, 2$^+$ cells. Longitudinal analysis of polyfunctional BCG-specific CD4$^+$ T-cells shows Group 1 and Group 2 vaccinees to have higher probabilities of the 4$^+$ (IFN-γ/IL-2/TNF-α/MIP-1β), 3$^+$ (IFN-γ/IL-2/TNF-α, IFN-γ/IL-2/MIP-1β) and 2$^+$ (IFN-γ/IL-2) subsets compared to baseline (Figure 7, upper panel).

311 Among $CD8^+$ T-cells, BCG revaccination induced a robust increase in 3^+ subset
312 expressing three cytokines (IFN-γ/TNF-α/MIP-1β), 2^+ (combinations of IFN-γ, TNF-α,
313 MIP-1β) and 1^+ (IFN-γ, TNF-α, MIP-1β) cells in $IGRA^+$ Group 1 and $IGRA^-$ Group 2
314 subjects vs. unvaccinated controls (Group 3 and Group 4) in response to Ag85A
315 stimulation. BCG specific $CD8^+$ responses (1^+ and 2^+) were high for Group 1 and 2
316 vaccinees compared to baseline (Figure 7, lower panel).

317 The above whole blood data were extended using PBMC staining with a panel
318 measuring eight effector cytokines (IFN-γ, IL-2, TNF-α, MIP-1β, IL-17A, IL-17F, IL-22
319 and IL-10; Supplemental Table 1B). COMPASS analysis of PBMC data confirms the
320 enhanced Ag85A and BCG $CD4^+$ polyfunctional scores (PFS) noted in whole blood
321 and extends the data to include latency antigens (Figure 8). A cross sectional
322 analysis of whole blood data shows significantly higher Ag85A and BCG PFS scores
323 in Group 1 'vs' Group 3 (Figure 8A). At the PBMC level, these differences are
324 confirmed (Figure 8B), but in addition, we note higher PFS scores to BCG but not
325 Ag85A in Group 2 'vs' Group 4 subjects. We further demonstrate through analysis of
326 PBMC that Group 1 $IGRA^+$ vaccinees had significantly higher LTAg PFS scores
327 compared to unvaccinated controls (Figure 8B). These data collectively confirm that
328 BCG revaccination has the potential to boost Mtb-specific polyfunctional $CD4^+$ and
329 $CD8^+$ T-cells, in both $IGRA^+$ and $IGRA^-$ young adults with the boosting effect being
330 more consistent across all antigens tested in $IGRA^+$ subjects.

331 ***BCG revaccination enhances Mtb-specific Th17 responses***

332 Our previous studies highlight a key potential role of $CD4^+$ Th17 cells in Mtb infection
333 with functional differences noted between subjects with latent TB and TB disease
334 (49). Thus, Mtb-latency antigen-specific IL-10^+ regulatory Th17 cells expressing IL-
335 17A, IL-17F and IL-22 were significantly higher in subjects with latent TB compared
336 to those with active TB disease. By contrast, subjects with TB disease had

337 significantly higher numbers of Mtb-specific IL-17A or IL-17F or IL-22 cells that co-
338 expressed IFN-γ but not IL-10, indicating a shift to an Mtb-specific Th17 pro-
339 inflammatory $CD4^+$ T-cells during disease, with this shift being best revealed by $CD4^+$
340 T-cells specific for the DosR latency antigens, rather than the commonly studied
341 secretory mycobacterial antigens (49). Therefore, we sought to determine if BCG
342 revaccination could boost circulating frequencies of Mtb-specific $IL17^+$ and $IL\text{-}10^+$
343 total and double-positive Th17 cells in both $IGRA^+$ and $IGRA^-$ vaccinees, comparing
344 PBMC responses specific for Ag85A, BCG and latency antigens.

345 First, we show in Figure 9 (upper panel), representative dot plots of $CD4^+$ T-cells
346 expressing Th17 cytokines at 34 weeks (T5) post-vaccination in BCG stimulated
347 PBMCs from a Group 1 and Group 3 subject (see Supplemental Figure 4 for
348 immunostaining of unstimulated control sample). Figure 9 (lower panel) summarises
349 total frequencies of effector $CD4^+$ T-cells that express IL-17A, IL-17F, IL-22, IFN-γ
350 and IL-10 and highlights all these cytokine positive cells to be significantly higher in
351 $IGRA^+$ vaccinees (Group 1) compared to unvaccinated $IGRA^+$ controls (Group 3)
352 especially to Ag85A and BCG stimulation. LTAg responses were similar but not
353 significantly different for IL-17A (Figure 9, lower panel). We also record significantly
354 higher frequencies of total $CD4^+$ T-cells expressing IL-17A, IL-17F, IL-22 and IL-10 in
355 $IGRA^-$ Group 2 vaccinees compared to Group 4 unvaccinated $IGRA^-$ controls (Figure
356 9, lower panel). These data provide strong evidence that BCG revaccination has the
357 potential to boost Mtb-specific Th17 responses in both $IGRA^+$ and $IGRA^-$ subjects.

358 We next determined the frequencies of double-positive specific $CD4^+$ T-cells that co-
359 expressed IL-17A or IL-17F or IL-22 with either IFN-γ (pro-inflammatory Th17) or IL-
360 10 (regulatory Th17), with representative gating data shown in Supplemental Figure
361 5 and 6 highlighting these double positive cells to be a minor subset, confirmed by
362 backgating to be viable cells. Figure 10 shows significantly higher frequencies of IL-
363 $17F^+IL\text{-}10^+$ cells specific for Ag85A and BCG in both Group 1 $IGRA^+$ and Group 2

IGRA$^-$ vaccinees relative to unvaccinated controls, with higher proportion of responders in Group 1 (50-80%) and Group 2 (20-40%) compared to unvaccinated Group 3 (10%) and 4 (10%), respectively. LTAg-specific IL-17F/IL-10 was also higher than unvaccinated controls, but only in Group 1 IGRA$^+$ vaccinees. With the exception of Ag85A in Group 1 vaccinees, revaccination did not enhance Th17 proinflammatory cells that co-expressed IL-17A or IL-17F or IL-22 with IFN-γ (Figure 10). Thus, the extent to which specific cells were upregulated differed by antigen specificity and were evident in some but not all vaccinees. These data demonstrate that BCG revaccination has the potential to enhance a minor Mtb-specific anti-inflammatory, regulatory Th17 subset in both IGRA$^+$ and IGRA$^-$ subjects.

BCG revaccination-induces innate specific cells

A previous study (48) had reported that BCG revaccination in adults transiently induces BCG-reactive γδ$^+$, CD56$^+$ NKT-like, CD56^{dim} and CD56^{hi} NK cells that express IFN-γ in IGRA$^+$ subjects. We therefore evaluated whether BCG revaccination modulated the frequencies and function of innate lymphocyte populations. A representative example of the flow cytometric gating strategy to analyse these cells is shown in Supplemental Figure 7. Revaccination induced significant expansion of Ag85A reactive innate effectors (γδ, CD56^{br} NK cells) above baseline T0 responses in both Group 1 IGRA$^+$ and Group 2 IGRA$^-$ vaccinees and NKT-cells in Group 1 only but not Group 3 and 4 unvaccinated controls (Figure 11) with the boosting effect ranging from 2-10-fold depending on the innate effector subset and was more consistent (in terms of proportion of vaccinees responding) in Group 1 IGRA$^+$ subjects. BCG reactive innate effectors (γδ, CD56^{dim}NK, CD56^{br} NK and NKT-cells) were significantly boosted at T5 (2-10-fold) above baseline T0 only in Group 1 IGRA$^+$ and not in Group 2 IGRA$^-$ vaccinees. Interestingly, the pattern of induction of these innate subsets was similar to the induced adaptive response (Figure 3 and 4). Thus, IFN-γ$^+$ innate lymphocytes induced by Ag85A re-stimulation peaked at T2 (4 weeks)

391 post revaccination, whereas, those specific to BCG epitopes were observed later at
392 T5 (34 weeks) post revaccination. These data highlight the potential of BCG to boost
393 innate Mtb-reactive cells in both Group 1 and Group 2 $IGRA^{+}$ and $IGRA^{-}$ subjects.
394
395

Discussion

We provide the first detailed evidence of the impact of BCG revaccination on Mtb-specific T-cell immunity in young adults from a TB endemic region of India. Our work confirms and extends in particular the report of Suliman et al on immune stimulating effects of BCG revaccination of young adults with latent TB living in South Africa (48). Novel aspects of our work include: (i) detailed investigation of polyfunctional Mtb-specific T-cells including up to 256 immune subsets; (ii) focused analysis of Mtb-specific pro-inflammatory as well as regulatory Th17 responses, the latter of which are highlighted to be of increasing importance in anti-TB immunity, based on our work and that of others (49, 50), and (iii) comparative longitudinal analysis of vaccine-induced responses in both $IGRA^+$ 'vs' $IGRA^-$ subjects, in the absence of anti-TB treatment.

The strong evidence we provide that BCG revaccination can boost polyfunctional Th1/Th17 and innate effectors in subjects living with latent TB in the absence of INH treatment distinguishes our study from that of the Suliman et al study (48), where TST^+ subjects were randomised into two arms: one receiving BCG revaccination after INH and the other receiving BCG revaccination first and then INH. In the Suliman et al study (48), immune responses did not differ between these treatment groups implying pre-treatment with INH does not interfere with BCG revaccination potency. In this paper we asked a different question: whether BCG revaccination can boost anti-TB immunity in the absence of INH treatment altogether. The fact that we demonstrate this to be the case is important as current thinking proposes that underlying infection with Mtb or cross-reactive NTM responses (10-13, 17) can potentially blunt responses to BCG revaccination. Hence most BCG revaccination studies have focussed on subjects without Mtb infection ($IGRA^-$) or latent TB subjects

(IGRA$^+$) after INH. IGRA$^+$ individuals live with a considerably higher risk of succumbing to active TB (52). The results from our study show that Ag85A, BCG and LTAg-specific specific CD4$^+$ and CD8$^+$ T-cell responses are boosted to a greater extent in IGRA$^+$ rather than IGRA$^-$ individuals. Thus, in India BCG revaccination might be more beneficial to the more susceptible IGRA$^+$ population. This has implications for future BCG revaccination/other TB vaccination strategies.

All the antigens tested in this study (Ag85A, TB10.4 and DosR regulon encoded latency antigens) are encoded by BCG (53-56). Our own and previous studies have shown that BCG vaccination does not lead to generation of potent immune responses against DosR encoded latency antigens (49, 55, 56). However, we show in this paper that DosR specific T-cell responses can be boosted by BCG revaccination of young Indian adults. Ag85A and TB10.4 are both vaccine candidates and have shown protection against *M. tuberculosis* infection in animal models (57-60). In addition, Ag85A was found to be well tolerated in BCG vaccinated infants and significantly boosted Ag85A-specific Th1 and Th17 responses (61). H4:IC31, another candidate vaccine comprising Ag85B and TB10.4 was tested in adolescents and found to be immunogenic and capable of reducing the rate of sustained Quantiferon (QFT) conversion (45). DosR encoded latency antigens, which we and others show to distinguish subjects with latent and active TB individuals (49, 62) was also shown to have protective efficacy in NHP, most likely via induction of CD4$^+$ as well as CD8$^+$ T-cells. In this context, whether BCG revaccination of young IGRA$^+$ adults can induce protective immunity and reversion of IGRA$^+$ untreated subjects to an IGRA$^-$ state remains to be tested.

The importance of probing adaptive T-cell responses to Mtb antigens is based on significant data from mouse knockout models demonstrating the dominant role of $CD4^+$, and to a lesser extent $CD8^+$ Mtb-specific T-cells in protection against Mtb infection following immunization with BCG (63, 64). While Suliman et al (48) reported peak responses at 3 weeks post revaccination, we report peak BCG responses to occur later, at 34 weeks post revaccination. This disparity may reflect differences in the BCG strains used. Further, the TST^+ subjects recruited to the Suliman et al study (48) received INH whereas $IGRA^+$ subjects recruited to our study remained treatment naive. We also show significantly enhanced Ag85A responses in both $IGRA^+$ and $IGRA^-$ revaccinated subjects that transiently peaked at T2 (4 weeks) post revaccination, consistent with the observation that Ag85A responses following BCG vaccination in infants (61) and in murine models are transient based on low antigen load (65). Comparative analysis of the boosting effect in $IGRA^+$ versus $IGRA^-$ subjects revealed a more marked effect in $IGRA^+$ subjects, who had a higher baseline specific T-cell response; consequently, the more efficacious boosting effect of BCG revaccination may be due to expansion of pre-existing memory T-cells. Beyond analysis of T-cell responses and in keeping with the findings of Suliman et al., our study also shows that NK, NKT and γδ T-cell BCG-specific responses are boosted in $IGRA^+$ vaccinees. These data provide strong evidence that BCG revaccination has the potential to boost both the innate and adaptive arms of the immune system in adults in the time frame of 9 months/34 weeks post vaccination.

Beyond IFN-γ and/or IL-2 specific T-cell responses, we used the statistically robust COMPASS analysis to probe polyfunctional T-cell responses encompassing 8 effectors representing a total of 256 immune subsets (66). Polyfunctional Mtb-specific $CD4^+$ T-cells simultaneously expressing IFN-γ, IL-2, and TNF-α in blood are implicated in anti-TB immunity (67, 68) and shown to be critical in modulating

vaccine-mediated immunity in murine re-challenge studies (69-72). Further, we previously showed Mtb-specific polyfunctional cells expressing up to 4 cytokines to be associated with controlled latent infection, (49). Herein, we report that BCG revaccination significantly boosts circulating frequencies of $CD4^+$ and $CD8^+$ polyfunctional T-cells expressing up to 4 effectors (IFN-γ, IL-2, TNF-α, IL-17A) specific to Ag85A and BCG, in both $IGRA^+$ and $IGRA^-$ subjects. In addition, we conducted a more focussed analysis of Th17 cells, which have emerged as potential correlates of protective immunity in human studies (see 49) and in vaccine-induced protection against TB (50, 73-76). Th17 subsets that express pro-inflammatory cytokines (IL-17A/IL-17F/IL-22 in combination with IFN-γ) are associated with pathogenesis of several chronic disease conditions; in contrast, subsets that express Th17 cytokines in combination with IL-10 can protect against disease pathology and therefore implicated to be protective in chronic conditions (77). In this manuscript, we demonstrate that BCG revaccination significantly boosted a minor population of anti-inflammatory $CD4^+$ T-cells specific for Ag85A, BCG and LTAg that co-expressed IL-17F and IL-10 in a proportion of $IGRA^+$ and $IGRA^-$ vaccinees, whilst the boosting effect of pro-inflammatory cells expressing IFN-γ and IL-17 was weaker and only noted to Ag85A stimulation. These data call for further studies to probe the potential efficacy of BCG revaccination in regulating Th17 responses.

There is evidence for at least three potential mechanisms for the immunogenic function of BCG. First, BCG revaccination may expand pre-existing memory T-cells. Continuous T-cell stimulation by underlying infection is known to maintain a higher basal Mtb-specific adaptive T-cell response in $IGRA^+$ compared to $IGRA^-$ subjects, and BCG revaccination may induce the proliferation of these pre-existing cells. Secondly, BCG may boost T-cell responses through immunomodulatory anti-inflammatory effects, especially through IL-10 upregulation (78). This is consistent with our observation that BCG revaccination can induce total IL-10 Mtb-specific $CD4^+$

T-cells and is supported by data on mucosal BCG vaccination in mice, which induces airway $CD103^{-}CD69^{+}CD4^{+}$ memory T-cells, likely to be tissue resident memory (TRM) cells, that represent a heterogeneous population comprising of $Foxp3^{+}$- or $T\text{-}bet^{+}$- T-cell subsets, producing IL-10 in addition to Th1 response (79). Thirdly, BCG may regulate innate immune cells in a pathogen specific manner and thereby provide resistance to secondary infections through "trained immunity" through potential epigenetic changes (80-82). Suliman et al reported that BCG-reactive $CD3^{+}CD56^{+}$ NKT-like cells as well as $CD56^{hi}CD16^{lo}$ and $CD56^{dim}CD16^{+}$ NK cells to persist for up to 1 year post BCG revaccination, suggesting memory function akin to conventional T-cells (48). We too report an increase of $CD3^{+}CD56^{+}$ NKT and $CD56^{br}$ and $CD56^{br}$ NK cells in BCG revaccinated $IGRA^{+}$ subjects in response to Ag85A and BCG stimulation at 4 and 34 weeks post revaccination, confirming a further mechanism of the beneficial effects of BCG revaccination through potential regulation of innate immunity.

The importance of the immunostimulatory effects of BCG revaccination has to be placed in the broader context of immune components that may protect against Mtb infection. This has fundamental challenges because dominant immune responses elicited by vaccines in blood may not predict necessary effector responses in lung tissue following Mtb exposure by inhalation. Murine studies demonstrate that Mtb infects phagocytes with diverse phenotypes and that infected myeloid dendritic cells migrate from lungs to local lymph nodes early in infection, where T-cell activation can occur (83). Thus, a desirable vaccine might elicit innate immune activation of local myeloid cells that can kill the bacteria in the lung as well as T-cells that can rapidly enter the lung parenchyma, recognize infected cells and destroy them (84, 85). This calls for further studies on key immune innate and adaptive phenotypes post-immunization including specific T-cells that are imprinted to traffic to lung tissue. Our

data on the boosting effects of BCG in a TB endemic region of South India together with the reported efficacy of BCG revaccination in prevention of infection in South Africa (45) provide a rational basis for further mechanistic analysis of the immunostimulatory effects of BCG in divergent populations based on geography and NTM exposure.

METHODS

Study population

A total of 200 young adults (age 18-28 years), mostly nursing college students from Madanapalle, South India, a TB endemic area, were prospectively recruited between January 2014 and December 2015 for the vaccination study primarily by college-wide informational seminars. All participants were confirmed as HIV-1 seronegative and BCG vaccinated at birth and had a visible BCG scar. Relevant clinical information of study participants was documented in a proforma and is summarized in Table 1 and Supplemental File 1. Blood from study participants was screened for Mtb infection by the standard QuantiFERON TB Gold In-tube test (Qiagen, Germany) performed at the blood collection centre in Madanapalle and were classified as either interferon gamma release assay (IGRA) positive or negative (86). $IGRA^+$ subjects were enrolled only if they had no known TB disease and had not received preventive/curative therapy for TB in the past. Two hundred subjects were enrolled and then divided into four clinical groups based on their IGRA result and randomization to receive BCG (Figure 1A).

Vaccination

BCG vaccine (TUBERVAC, Russian BCG strain manufactured at Serum Institute of India, Pune) used widely in the Indian national immunization program was administered intradermally at day 0 at an adult dose of 2–8 x 10^5 CFU in participants from group 1 ($IGRA^+$, N=28) and group 2 ($IGRA^-$, N=30). Group 3 ($IGRA^+$ N=24) and Group 4 ($IGRA^-$ N=23) were not BCG revaccinated and served as controls for Groups 1 and 2 respectively. As greater than 90% of the volunteers recruited were nursing students, Hepatitis B vaccination (HBV) was given to fulfill their immunization requirements as health care workers as they are at high risk for HBV; additionally, this vaccination enhanced compliance to our longitudinal BCG revaccination study

protocol. All participants (irrespective of whether they received BCG or not) therefore received HBV vaccine at 4 (T2), 10 (T4) and 30 weeks post-BCG vaccination. Blood was collected from participants at days 0 (T0) and 3, and at weeks 4 (T2), 5 (T3), 10 (T4) and 34 (T5) post-BCG vaccination (Figure 1, A and B). Some vaccinees, after BCG vaccination, reported minor side effects which included itching/rash/pain at the site of vaccination, mild fever, cough and headache (Supplemental File 1). No serious side effects were reported and none of the participants become active TB^+ during the entire duration of study.

Antigen and antibody reagents

Peptide pools that spanned the amino acid sequence of mycobacterial proteins Ag85A, TB10.4 and HBV surface antigen were constructed. Each peptide was 15 amino acids and overlapped by 12 amino acids with the next sequential peptide (BIoSynthesis) and was 1 μg/ml as previously described (87). Four DosR regulon-encoded latency antigens (Rv1733c, Rv1737c, Rv2029 and Rv2628) were synthesized as recombinant proteins at the Department of Infectious Diseases, Leiden University Medical Center, The Netherlands. BCG Vaccine (TUBERVAC) was reconstituted in RPMI 1640 (final concentration 1.2-33.0 x 10^6 CFU/ml blood). All intracellular cytokine staining (ICS) assay stimulations were performed in the presence of anti-CD28/CD49d co-stimulatory antibodies (at 1 μg/ml, BD Biosciences). Fluorochrome conjugated monoclonal antibodies to cell surface and intracellular markers used in flow cytometry assays are listed in Supplemental Table 1, A and B. Antibodies were sourced from BD Biosciences, BioLegend and eBioscience (Supplemental Table 1, A and B).

Peripheral blood mononuclear cell isolation: Anticoagulated blood (16 ml) was collected in ACD tubes (BD, Franklin Lakes NJ, USA) and peripheral blood mononuclear cells (PBMCs) were isolated using ACCUSPIN (Sigma-Aldrich) tubes by density centrifugation following manufacturer's instructions. Blood was diluted two-

602 fold with PBS (Gibco by Life Technologies, Washington, DC, USA) + 2% FBS
603 (Gibco), pipetted into ACCUSPIN tubes pre-filled with Histopaque 1077 and
604 centrifuged at 1000g for 15 minutes at room temperature without deceleration.
605 PBMCs from the buffy coat were washed twice with PBS + 2% FBS, then
606 resuspended at 5 x 10^6 cells/mL in cryopreservation medium (90% FBS and 10%
607 DMSO) and incubated overnight at -80°C (in Mr. Frosty™ freezing container;
608 Nalgene, USA) and were stored in liquid nitrogen until further analyses.

609 **Intracellular cytokine staining (ICS) assay and multiparameter flow cytometry**

610 ***Whole blood:*** Heparinized whole blood was collected from participants and
611 processed within 30-45 min of phlebotomy, as previously described (88). Briefly, 400
612 μl of blood was pipetted into Sarstedt tubes and stimulated with peptide pools (1
613 μg/ml per peptide) or with BCG (2.4 – 60 x 10^4 CFU/ml) together with anti-
614 CD28/CD49d costimulatory mAbs at 0.5 μg/ml. Phytohemagglutinin (PHA) (Remel,
615 Thermo Fisher Scientific, UK) was used as a positive mitogen control and culture
616 medium with anti-CD28/CD49d was used as unstimulated negative control. Blood
617 was incubated at 37˚C for a total of 12 h, and Brefeldin A (Sigma-Aldrich) at a
618 concentration of 10 μg/ml was added in the final 5 h of stimulation. After stimulation,
619 blood was treated with 2 μM EDTA (Sigma), RBCs were lysed with 4.5 ml 1X FACS
620 Lysing solution (BD), and fixed cells were transferred to liquid nitrogen in freezing
621 medium containing 10% DMSO, 40% FCS, and 50% RPMI 1640. For staining,
622 cryopreserved whole-blood samples were thawed in a water bath at 37°C for 2 min.
623 Thawed cells were transferred to labelled tubes containing 2 mL of PBS and were
624 centrifuged at 2000 rpm for 5 min. Cells were then stained with a 50 μl cocktail
625 containing cell surface antibodies for 30 min at room temperature (RT) in the dark.
626 Next, cells were washed with PBS, permeabilized with 200 μl 1X Perm/Wash solution
627 (BD Biosciences) and incubated at RT for 20 min. Pelleted cells were immediately

stained with a 50 µl cocktail containing antibodies against intracellular markers for 30 min at RT. Cells were washed and resuspended in 100 µl of 1% paraformaldehyde (Electron Microscopy Sciences, USA) for flow cytometry analysis.

PBMC: ICS assay with cryopreserved, antigen-stimulated PBMCs was performed as previously described (89). Cryopreserved PBMC samples were rapidly thawed in a 37°C water bath, transferred to 15 ml tubes containing ~ 3 ml PBS and centrifuged at 2000 rpm for 5 min at RT. One million cells resuspended in 200 µL culture medium [RPMI-1640 (GIBCO, Invitrogen) supplemented with 10% FCS (GIBCO), 100 U/ml penicillin and 100 µg/ml streptomycin, (Sigma)] were seeded per well in 96-well round-bottom plates (Costar) and stimulated with either Ag85A peptide pools (1 µg/ml) or recombinant latency proteins (10 µg/ml) or BCG (2.4 – 60 x 10^4 CFU/ml) or PHA (1 µg/ml) at 37°C and 5% CO_2. After 4 h of stimulation, brefeldin A (10 µg/ml) was added. On the next day, PBMC were washed after incubation with EDTA and first stained with 5 µl Live/Dead Aqua (Invitrogen) followed by a 50 µl cell surface staining cocktail for 30 min at RT in the dark. Cells were then fixed for 20 min with 100 µl 1X FACS lysis buffer and permeabilized with 200 µl 1X BD Perm/Wash buffer for 20 min. PBMCs were washed and incubated for 30 min at RT in the dark with a 50 µl intracellular staining cocktail. Finally, cells were washed with 150 µl Perm/Wash buffer and resuspended in ~100µl of 1% paraformaldehyde for flow cytometry analysis.

Flow cytometry analysis: Samples were acquired on BD FACSAria™ Fusion flow cytometer and BD FACSDiva™ version 8.0.1 software (BD Biosciences). Cytometer Setting and Tracking (CST) beads (BD Biosciences) were acquired before each experiment to ensure consistency across all experiments. Stained samples were acquired with a standard stopping gate set at 1 x 10^5 $CD3^+$ lymphocytes. Unstained cells and single-stained beads (eBioscience) were used for calculating the

compensation matrix. Data was analyzed and Boolean cytokine combinations were generated using FlowJo version 9.9.4 software (Treestar, Ashland, OR). Background subtractions were performed in Pestle version 1.8.

COMPASS application of flow cytometry data: Cell counts were analyzed using the COMbinatorial Polyfunctionality Analysis of Antigen-Specific T-cell Subsets (COMPASS) algorithm as described (66). Briefly, COMPASS is a statistical model developed for high-dimensional flow cytometry data analysis that can detect antigen-specific changes across all observable functional T-cell subsets, without the need to limit the analysis to very specific subsets based on expected biological significance. COMPASS was applied to the three antigens in two ($CD4^+$ and $CD8^+$) T-cell subsets leading to 20 analyses. Each analysis was unbiased and considered all of the 31 possible cytokine functions (defined as Boolean combination). To evaluate differences in polyfunctionality between groups, a linear model estimating the group wise mean polyfunctionality scores was fit to each antigen and the difference between $IGRA^+$ and other groups was tested (Wald test, null: $\hat{\beta}_{group} - \hat{\beta}_{IGRA} = 0$, two-sided test). Resulting p-values were adjusted for multiple testing (across all 60 tests and models) to control the FDR (false discovery rate) using the method of Benjamini & Hochberg (90). Significant differences were designated at the 5% FDR level. Magnitudes of T-cell responses were calculated independent of COMPASS as the maximum of zero or the proportion of gated events in the stimulated condition minus the proportion of gated events in the unstimulated condition.

Hepatitis B ELISA: Antibodies to hepatitis B surface antigen were measured in plasma at 1:2 dilution using the anti-HepB surface antigen ELISA kit from XpressBio Life Science Products (catalogue number WB2896, Frederick, MD). All study participants received three doses of HBV (Figure 1). However, we did not notice any

benefits of BCG vaccination on Hep B responses in our study as all subjects across all 4 groups in our study had comparable peak Hep B antibody titers at T5 (week 35) post third Hep B vaccination with no significant differences of the peak response over time points tested (Supplemental Figure 8).

Statistical Analysis: All antigen-stimulated wells were adjusted for nonspecific responses by background subtraction (media alone). Statistical analyses were performed and graphs were created using GraphPad Prism software version 6.0.7 (GraphPad, La Jolla, CA). Paired longitudinal comparisons within the same group were done using the two-sided Wilcoxon matched pairs signed rank test. Comparisons across two treatment groups were done using unpaired Mann–Whitney U test. One-way analysis of variance (ANOVA) test, followed by Bonferroni post-hoc tests for multiple comparisons was used to compare three cytokines between two groups. Differences were considered statistically significant for p-value <0.05. Box-and-whisker plot depicts the interquartile range with median bars and with whiskers depicting minimum and maximum values. Scatter plots depict median values with range. In Figures 3C, 3G, 4C and 4G mean ± SD was plotted.

Study approval

This study was performed in accordance with the relevant guidelines and regulations stated in the Declaration of Helsinki and approved by the Ethical Review Committee of Arogyavaram Medical Centre (Madanapalle, Andhra Pradesh, India, IEC - AMC 2014/5). All study volunteers provided written consent prior to enrolment. Study protocols were approved by institutional review boards of Arogyavaram Medical Centre.

Author contributions

MJM and AV conceived the project. SR, AA, SDeR. and AV designed the experiments. SR and AA contributed equally. SR and AA performed the immunology experiments and analysed the data. SDeR and VA helped with flow cytometer instrument set up, acquisition, and data analysis. BKS and PNS helped with processing of blood from clinical cohorts. GF performed the main bioinformatic and immuno-informatic analyses. GD and JK were clinical investigators. WB and CJ collected clinical samples, provided the patient details and wrote the clinical methodology for the manuscript. THMO supplied the latency antigen recombinant proteins. SR, AA and AV wrote the manuscript. SDeR, THMO, MJM and AV edited the manuscript.

Conflict of Interest Statement

The authors declare that the research was conducted in the absence of any commercial or financial relationships that could be construed as a potential conflict of interest.

Acknowledgments

The authors thank the volunteers for participating in this study and acknowledge the contributions of clinical research workers at Arogyavaram Medical Centre and St John's Research Institute. This work was funded principally by DBT-NIH (BT/MB/Indo-US/HIPC/2013) to AV and JM and also supported by the National Institute of Allergy and Infectious Diseases of the US National Institutes of Health (UM1 AI 068618). We acknowledge additional funding for antigen synthesis by EC HORIZON2020 TBVAC2020 and EC FP7 EURIPRED (FP7-INFRA-2012 Grant Agreement No. 312661) to AV and THMO.

REFERENCES

1. World Health Organization (WHO). Global Tuberculosis Report 2018. www.who.int/tb/publications/global_report/en/ Date last accessed: May 10, 2019. Date last updated: 2017.
2. Floyd K, Glaziou P, Zumla A, Raviglione M. The global tuberculosis epidemic and progress in care, prevention, and research: an overview in year 3 of the End TB era. *Lancet Respir Med*. 2018;6(4):299-314.
3. World Health Organization (WHO). Latent TB Infection: Updated and consolidated guidelines for programmatic management. https://www.who.int/tb/publications/2018/latent-tuberculosis-infection/en/
4. World Health Organization. BCG vaccine: WHO position paper, February 2018 - Recommendations. *Vaccine*. 2018;36(24):3408-3410.
5. Andersen P, Doherty TM. The success and failure of BCG - implications for a novel tuberculosis vaccine. *Nat Rev Microbiol*. 2005;3(8):656-662.
6. Mangtani P, et al. Protection by BCG vaccine against tuberculosis: a systematic review of randomized controlled trials. *Clin Infect Dis*. 2014;58(4):470-480.
7. Moliva JI, Turner J, Torrelles JB. Immune responses to BCG vaccination: why do they fail to protect against *M. tuberculosis*? *Front Immunol*. 2017;8:407.
8. Dockrell HM, Smith SG. What have we learnt about BCG vaccination in the last 20 years? *Front Immunol*. 2017;8:1134.
9. Roy A, et al. Effect of BCG vaccination against *M. tuberculosis* infection in children: systematic review and meta-analysis. *BMJ*. 2014;349:g4643.
10. Zodpey SP, Shrikhande SN. The geographic location (latitude) of studies evaluating protective effect of BCG vaccine and it's efficacy/effectiveness against tuberculosis. *Indian J Public Health*. 2007;51(4):205-210.

11. Brandt L, et al. Failure of the *M. bovis* BCG vaccine: some species of environmental mycobacteria block multiplication of BCG and induction of protective immunity to tuberculosis. *Infect Immun*. 2002;70(2):672-678.
12. Poyntz HC, Stylianou E, Griffiths KL, Marsay L, Checkley AM, McShane H. Non-tuberculous mycobacteria have diverse effects on BCG efficacy against *M. tuberculosis*. *Tuberculosis (Edinb)*. 2014;94(3):226–237.
13. Zimmermann P, Finn A, Curtis N. Does BCG vaccination protect against non-tuberculous mycobacterial infection? A systematic review and meta-analysis. *J Infect Dis*. 2018;218(5):679-687.
14. Kontturi A, Soini H, Ollgren J, Salo E. Increase in childhood nontuberculous mycobacterial infections after BCG coverage drop: a nationwide, population-based retrospective study, Finland, 1995-2016. *Clin Infect Dis.* 2018;67(8):1256-1261.
15. Abate G, Hamzabegovic F, Eickhoff CS, Hoft DF. BCG vaccination induces *M. avium* and *M. abscessus* cross-protective immunity. *Front Immunol*. 2019; 10:234.
16. Narayanan PR. Influence of sex, age & non-tuberculous infection at intake on the efficacy of BCG: re-analysis of 15-year data from a double-blind randomized control trial in South India. Indian *J. Med. Res*. 2006;123(2):119–124.
17. Valadas E. Nontuberculous mycobacteria: clinical importance and relevance to bacille Calmette-Guérin vaccination. *Clin Infect Dis*. 2004;39(4):457-458.
18. Orme IM. The Achilles heel of BCG. *Tuberculosis (Edinb)*. 2010;90(6):329-332.
19. Hesseling AC, Jaspan HB, Black GF, Nene N, Walzl G. Immunogenicity of BCG in HIV-exposed and non-exposed infants following routine birth or delayed vaccination. *Int J Tuberc Lung Dis*. 2015;19(4):454-462.
20. Geldmacher C, Zumla A, Hoelscher M. Interaction between HIV and *M. tuberculosis*: HIV-1-induced $CD4^+$ T-cell depletion and the development of active tuberculosis. *Curr Opin HIV AIDS*. 2012;7(3):268-275.

21. Pawlowski A, Jansson M, Sköld M, Rottenberg ME, Källenius G. Tuberculosis and HIV co-infection. *PLoS Pathog*. 2012;8(2):e1002464.
22. Ahmed A, Rakshit S, Vyakarnam A. HIV-TB co-infection: mechanisms that drive reactivation of *M. tuberculosis* in HIV infection. *Oral Dis*. 2016;22 Suppl 1:53-60.
23. Hawn TR, et al. Tuberculosis vaccines and prevention of infection. *Microbiol Mol Biol Rev*. 2014;78(4):650- 671.
24. Aerosol Vaccines for Tuberculosis Workshop Summary Group. Developing aerosol vaccines for *M. tuberculosis*: Workshop proceedings: National Institute of Allergy and Infectious Diseases, Bethesda, Maryland, USA, April 9, 2014. *Vaccine*. 2015;33(26):3038-3046.
25. Hansen SG, et al. Prevention of tuberculosis in rhesus macaques by a cytomegalovirus based vaccine. *Nat Med*. 2018;24(2):130-143.
26. Kaufmann SH, Weiner J, von Reyn CF. Novel approaches to tuberculosis vaccine development. *Int J Infect Dis. 2017*;56:263-267.
27. Satti I, et al. Safety and immunogenicity of a candidate tuberculosis vaccine MVA85A delivered by aerosol in BCG-vaccinated healthy adults: a phase 1, double-blind, randomized controlled trial. *Lancet Infect Dis*. 2014;14(10):939-946.
28. Barreto ML, Pereira SM, Ferreira AA. BCG vaccine: efficacy and indications for vaccination and revaccination. *J Pediatr (Rio J).* 2006;82(3 Suppl):S45-S54.
29. Karonga Prevention Trial Group. Randomised controlled trial of single BCG, repeated BCG, or combined BCG and killed *M. leprae* vaccine for prevention of leprosy and tuberculosis in Malawi. *Lancet*. 1996;348(9019):17–24.
30. Leung CC, Tam CM, Chan SL, Chan-Yeung M, Chan CK. Efficacy of the BCG revaccination programme in a cohort given BCG vaccination at birth in Hong Kong. *Int J Tuberc Lung Dis*. 2001;5(8):717-723.
31. Roth AE, et al. Effect of revaccination with BCG in early childhood on mortality: randomised trial in Guinea-Bissau. *BMJ*. 2010;340:c671.

843 32. Tala-Heikkil MM, Tuominen JE, Tala EO. BCG revaccination questionable with
844 low tuberculosis incidence. *Am J Respir Crit Care Med*. 1998;157(4 Pt 1):1324-
845 1327.
846 33. Rahman M, Sekimoto M, Hira K, Koyama H, Imanaka Y, Fukui T. Is BCG
847 revaccination necessary for Japanese children? *Prev Med*. 2002;35(1):70-77.
848 34. Kubit S, Czajka S, Olakowski T, Piasecki Z. Effectiveness of BCG vaccination.
849 *Pediatr Pol*. 1983;58(10):775-781.
850 35. Fjällbrant H, Ridell M, Larsson LO. Primary vaccination and revaccination of
851 young adults with BCG: a study using immunological markers. *Scand J Infect*
852 *Dis*. 2007;39(9):792-798.
853 36. Whelan KT, et al. Safety and immunogenicity of boosting BCG vaccinated
854 subjects with BCG: comparison with boosting with a new TB vaccine, MVA85A.
855 *PLoS One*. 2009;4(6):e5934.
856 37. Dourado I, Rios MH, Pereira SM, Cunha SS, Ichihara MY. Rates of adverse
857 reactions to first and second doses of BCG vaccination: results of a large
858 community trial in Brazilian school children. *Int J Tuberc Lung Dis*. 2003;
859 7(4):399-402.
860 38. Dantas OM, et al. A case-control study of protection against tuberculosis by
861 BCG revaccination in Recife, Brazil. *Int J Tuberc Lung Dis*. 2006;10(5):536-541.
862 39. Rodrigues LC, et al. Effect of BCG revaccination on incidence of tuberculosis in
863 school-aged children in Brazil: the BCG-REVAC cluster-randomised trial. *Lancet.*
864 2005;366(9493):1290-1295.
865 40. Barreto ML, et al. Evidence of an effect of BCG revaccination on incidence of
866 tuberculosis in school-aged children in Brazil: second report of the BCG-REVAC
867 cluster-randomised trial. *Vaccine*. 2011;29(31):4875-4877.
868 41. Barreto ML, et al. Causes of variation in BCG vaccine efficacy: examining
869 evidence from the BCG REVAC cluster randomized trial to explore the masking
870 and the blocking hypotheses. *Vaccine*. 2014;32(30):3759-3764.

871 42. Hatherill M, et al. Safety and reactogenicity of BCG revaccination with isoniazid
872 pre-treatment in TST positive adults. *Vaccine.* 2014;32(31):3982-3988.
873 43. Ahmad NA, et al. Bacille Calmette-Guerin (BCG) Revaccination: Is it Beneficial
874 for Tuberculosis Control? 2013; 2: 656. doi:10.4172/scientificreports.656
875 44. Dye C. Making wider use of the world's most widely used vaccine: BCG
876 revaccination reconsidered. *J R Soc Interface*. 2013; 10(87):20130365.
877 45. Nemes E, et al; C-040-404 Study Team. Prevention of *M. tuberculosis* infection
878 with H4:IC31 vaccine or BCG revaccination. *N Engl J Med.* 2018;379(2):138-
879 149.
880 46. Oliveira ES, Marinho JM, Barbosa T; study group. Interferon-gamma production
881 by mononuclear cells in BCG-revaccinated healthy volunteers predicted long-
882 term anti-mycobacterial responses in a randomized controlled trial. *Vaccine*.
883 2013;31(37):3778-3782.
884 47. Andersen A, et al. The immunological effect of revaccination with BCG vaccine
885 at 19 months of age. *Vaccine.* 2013;31(17):2137-2144.
886 48. Suliman S, et al. Bacillus Calmette-Guérin (BCG) Revaccination of adults with
887 latent *Mycobacterium tuberculosis* infection induces long-lived BCG-reactive NK
888 cell responses. *J Immunol*. 2016;197(4):1100-1110.
889 49. Rakshit S, et al. Circulating *M. tuberculosis* DosR latency antigen-specific,
890 polyfunctional regulatory IL-10^{+} Th17 CD4^{+} T-cells differentiate latent from active
891 tuberculosis. *Sci Rep*. 2017;7(1):11948.
892 50. Dijkman K, et al. Prevention of tuberculosis infection and disease by local BCG
893 in repeatedly exposed rhesus macaques. *Nat Med*. 2019;25(2):255-262.
894 51. Skjøt RL, et al. Epitope mapping of the immunodominant antigen TB10.4 and the
895 two homologous proteins TB10.3 and TB12.9, which constitute a subfamily of
896 the esat-6 gene family. *Infect Immun*. 2002;70(10):5446-5453.
897 52. Hatherill M, et al. BCG and New Preventive Tuberculosis Vaccines: Implications
898 for Healthcare Workers. *Clin Infect Dis*. 2016;62(Suppl 3):S262-S267.

899 53. Wiker HG, Harboe M. The antigen 85 complex: a major secretion product of
900 Mycobacterium tuberculosis. *Microbiol Rev*. 1992;56(4):648-661.
901 54. Belisle JT, Vissa VD, Sievert T, Takayama K, Brennan PJ, Besra GS. Role of
902 the major antigen of *Mycobacterium tuberculosis* in cell wall biogenesis.
903 *Science*. 1997;276(5317):1420-1422.
904 55. Coppola M, et al. New genome-wide algorithm identifies novel in-vivo expressed
905 *Mycobacterium tuberculosis* antigens inducing human T-cell responses with
906 classical and unconventional cytokine profiles. *Sci Rep*. 2016;6:37793.
907 56. Lin MY, et al. Lack of immune responses to *Mycobacterium tuberculosis* DosR
908 regulon proteins following *Mycobacterium bovis* BCG vaccination. *Infect Immun*.
909 2007;75(7):3523-3530.
910 57. Billeskov R, Elvang TT, Andersen PL, Dietrich J. The HyVac4 subunit vaccine
911 efficiently boosts BCG-primed anti-mycobacterial protective immunity. *PLoS*
912 *One.* 2012;7(6):e39909.
913 58. Elvang T, et al. CD4 and CD8 T-cell responses to the *M. tuberculosis* Ag85B-
914 TB10.4 promoted by adjuvanted subunit, adenovector or heterologous prime
915 boost vaccination. *PLoS One*. 2009;4(4):e5139.
916 59. Verreck FA, et al. MVA.85A boosting of BCG and an attenuated, PhoP deficient
917 *M. tuberculosis* vaccine both show protective efficacy against tuberculosis in
918 rhesus macaques. *PLoS One*. 2009;4(4):e5264.
919 60. Goonetilleke NP, McShane H, Hannan CM, Anderson RJ, Brookes RH, Hill AV.
920 Enhanced immunogenicity and protective efficacy against *Mycobacterium*
921 *tuberculosis* of BCG vaccine using mucosal administration and boosting with a
922 recombinant modified vaccinia virus Ankara. *J Immunol*. 2003;171(3):1602-1609.
923 61. Tameris MD, et al. Safety and efficacy of MVA85A, a new tuberculosis vaccine,
924 in infants previously vaccinated with BCG: a randomised, placebo-controlled
925 phase 2b trial. *Lancet*. 2013;381(9871):1021-1028.

926 62. Arroyo L, Marín D, Franken KLMC, Ottenhoff THM, Barrera LF. Potential of
927 DosR and Rpf antigens from *Mycobacterium tuberculosis* to discriminate
928 between latent and active tuberculosis in a tuberculosis endemic population of
929 Medellin Colombia. *BMC Infect Dis*. 2018;18(1):26.
930 63. Feng CG, Britton WJ. $CD4^+$ and $CD8^+$ T-cells mediate adoptive immunity to
931 aerosol infection of *Mycobacterium bovis* BCG. *J Infect Dis*. 2000;181(5):1846–
932 1849.
933 64. Moliva JI, Turner J, Torrelles JB. Immune responses to bcg vaccination: why do
934 they fail to protect against *Mycobacterium tuberculosis*? *Front Immunol*.
935 2017;8:407.
936 65. Moguche AO et al. Antigen availability shapes T-cell differentiation and function
937 during tuberculosis. *Cell Host Microbe*. 2017;21(6):695-706.e5.
938 66. Lin L, et al. COMPASS identifies T-cell subsets correlated with clinical
939 outcomes. *Nat Biotechnol*. 2015;33(6):610–616.
940 67. Marín ND, París SC, Rojas M, García LF. Functional profile of $CD4^+$ and $CD8^+$ T-
941 cells in latently infected individuals and patients with active TB. *Tuberculosis*
942 (Edinb). 2013;93(2):155–166.
943 68. Bhatt K, Verma S, Ellner JJ, Salgame P. Quest for correlates of protection
944 against tuberculosis. *Clin Vaccine Immunol*. 2015;22(3):258–266.
945 69. Yuan X, et al. A live attenuated BCG vaccine overexpressing multistage
946 antigens Ag85B and HspX provides superior protection against *Mycobacterium*
947 *tuberculosis* infection. *Appl Microbiol Biotechnol*. 2015;99(24):10587-10595.
948 70. Maggioli MF, et al. Increased TNF-α/IFN-γ/IL-2 and Decreased TNF-α/IFN-γ
949 production by central memory T-cells are associated with protective responses
950 against bovine tuberculosis following BCG vaccination. *Front Immunol*.
951 2016;7:421.

71. White AD, et al. Evaluation of the immunogenicity of *Mycobacterium bovis* BCG delivered by aerosol to the lungs of macaques. *Clin Vaccine Immunol*. 2015;22(9):992–1003.
72. Smith SG, Zelmer A, Blitz R, Fletcher HA, Dockrell HM. Polyfunctional CD4 T-cells correlate with in vitro mycobacterial growth inhibition following *Mycobacterium bovis* BCG-vaccination of infants. *Vaccine*. 2016;34(44):5298-5305.
73. Shen H, Chen ZW. The crucial roles of Th17-related cytokines/signal pathways in *M. tuberculosis* infection. *Cell Mol Immunol*. 2018;15(3):216-225.
74. Khader SA, Bell GK, Pearl JE, Fountain JJ, Rangel-Moreno J, Cilley GE. IL-23 and IL-17 in the establishment of protective pulmonary $CD4^+$ T-cell responses after vaccination and during *Mycobacterium tuberculosis* challenge. *Nat. Immunol*. 2007;8(4):369-377.
75. Wareham AS, et al. Evidence for a role for interleukin-17, Th17 cells and homeostasis in protective immunity against tuberculosis in cynomolgus macaques. *PloS One*. 2014;9(2):e88149.
76. Cruz A, et al. BCG vaccination-induced long-lasting control of *Mycobacterium tuberculosis* correlates with the accumulation of a novel population of $CD4^+$IL-17^+TNF^+IL-2^+ T-cells. *Vaccine*. 2015;33(1):85–91.
77. Alber G and Kamradt T. Regulation of Protective and Pathogenic Th17 Responses. *Current Immunology Reviews*. 2007;3:3-16.
78. Cavalcanti YV, Brelaz MC, Neves JK, Ferraz JC, Pereira VR. Role of TNFα, IFNγ, and IL10 in the development of pulmonary tuberculosis. *Pulm Med*. 2012;2012:745483.
79. Perdomo C, et al. Mucosal BCG vaccination induces protective lung-resident memory T-cell populations against tuberculosis. *MBio*. 2016;7(6):e01686-16.

80. Kleinnijenhuis J, et al. Long-lasting effects of BCG vaccination on both heterologous Th1/Th17 responses and innate trained immunity. *J Innate Immun*. 2014;6(2):152–158.
81. Kleinnijenhuis J, van Crevel R, Netea MG. Trained immunity: consequences for the heterologous effects of BCG vaccination. *Trans R Soc Trop Med Hyg*. 2015;109(1):29-35.
82. Sia JK, Georgieva M, Rengarajan J. Innate immune defenses in human tuberculosis: An overview of the interactions between *Mycobacterium tuberculosis* and innate immune cells. *J Immunol Res*. 2015;2015:747543.
83. Sada-Ovalle I, Chiba A, Gonzales A, Brenner MB, Behar SM. Innate invariant NKT-cells recognize *Mycobacterium tuberculosis*–infected macrophages, produce interferon-γ, and kill intracellular bacteria. *PLoS Pathog*. 2008;4(12):e1000239.
84. Rahman S, et al Compartmentalization of immune responses in human tuberculosis: few $CD8^+$ effector T-cells but elevated levels of $FoxP3^+$ regulatory T-cells in the granulomatous lesions. *Am J Pathol*. 2009;174(6):2211-2224.
85. Sakai S, et al. Cutting edge: control of *Mycobacterium tuberculosis* infection by a subset of lung parenchyma-homing CD4 T-cells. *J Immunol*. 2014;192(7):2965-2969.
86. Pattnaik S, John KR, Shalini E, Michael JS. Agreement between skin testing and QuantiFERON-TB Gold In-Tube assay (QFT-TB) in detecting latent tuberculosis infection among household contacts in India. *Indian J Tuberc*. 2012;59(4):214–218.
87. Horton H, et al. Optimization and validation of an 8-color intracellular cytokine staining (ICS) assay to quantify antigen-specific T-cells induced by vaccination. *J Immunol Methods.* 2007;323(1):39-54.

88. Kagina BM, et al. Qualification of a whole blood intracellular cytokine staining assay to measure mycobacteria-specific CD4 and CD8 T-cell immunity by flow cytometry. *J Immunol Methods*. 2015;417:22-33.
89. Smith SG, et al. TBVI TB Biomarker Working Group. Intracellular cytokine staining and flow cytometry: considerations for application in clinical trials of novel tuberculosis vaccines. *PLoS One*. 2015;10(9):e0138042.
90. Green GH, Diggle PJ. On the operational characteristics of the Benjamini and Hochberg False Discovery Rate procedure. *Stat Appl Genet Mol Biol*. 2007;6: Article 27.

FIGURE LEGENDS

Figure 1: Overall study design. (A) CONSORT flow diagram of participant recruitment and enrolment. (B) A diagrammatic representation of study design including schedule of vaccination and blood draw. Group 1 and Group 2 received BCG at day 0 (T0) and then three doses of HBV vaccine at weeks 4 (T2), 10 and 30 (T4). Group 3 and Group 4 did not receive BCG vaccine but three doses of HBV. Immunization time points are shown by blue arrows and the six blood sampling time points (T0-T5) are indicated by red arrows for all groups.

Figure 2: Baseline Mtb antigen-specific T-cell responses in whole blood of IGRA$^+$ vs. IGRA$^-$ subjects. Scatter plots of Ag85A, TB10.4 and BCG reactive IFN-γ and/or IL-2 expressing CD4$^+$ (upper panels) and CD8$^+$ (lower panels) T-cells in whole blood are shown after background subtraction at baseline in IGRA$^+$ vs. IGRA$^-$ subjects. Number of subjects in each group range from 38 to 42. Significant differences between groups were determined using the Mann–Whitney U test (*P* values < 0.05 are shown).

Figure 3: Longitudinal analysis reveals that BCG revaccination significantly enhances Ag85A- and BCG-specific IFN-γ and/or IL-2 CD4 T-cell responses in whole blood. Left hand panel shows ICS data for Ag85A and right-hand panel for BCG following *in vitro* stimulation of whole blood from BCG revaccinated and control subjects. Representative flow cytometry plots show IFN-γ and/or IL-2 cytokine positive CD4$^+$ T-cells after *in vitro* stimulation with either Ag85A (A) or BCG (E) at T0, T2 (A) and T5 (E). Total frequencies of Ag85A (B) and BCG-specific (F) IFN-γ and/or IL-2 cytokine-positive CD4$^+$ T-cells in all participants are shown after background

subtraction. Line graphs show changes in frequencies of specific $CD4^+$ T-cells over time in BCG revaccinated [Group 1 ($IGRA^+$, red, N = 19) and Group 2 ($IGRA^-$, blue, N = 18)] subjects and unvaccinated controls [Group 3 ($IGRA^+$, black, N = 18) and Group 4 ($IGRA^-$, brown, N = 18)]. P values for longitudinal samples were calculated by comparing each time point to baseline using the Freidman test and corrected for multiple comparisons using Dunn's test. Further, significant differences were determined using the Wilcoxon paired t-test pre and post vaccination. Bonferroni adjusted *P* value threshold of 0.02 was considered statistically significant. Median frequencies of Ag85A (C) and BCG (G) specific IFN-γ and/or IL-2 cytokine positive $CD4^+$ T-cells over time were compared between unvaccinated and revaccinated $IGRA^+$ and $IGRA^-$ subjects (Group 1 vs Group 3 and Group 2 vs Group 4). Mann-Whitney *U* test was used to determine significant differences between groups. $P < 0.05$ was considered significant. Analysis of CD45RA and CD27 expression was used to determine percentage distribution of naïve ($CD45RA^+CD27^+$,), central memory (CM, $CD45RA^-CD27^+$), effector memory (EM, $CD45RA^-CD27^-$) and terminally-differentiated T effector memory cells (TD, $CD45RA^+CD27^-$) Ag85A (D) and BCG (H)-specific IFN-γ and/or IL-2 $CD4^+$ T-cells in BCG-revaccinated [Group 1 ($IGRA^+$) and Group 2 ($IGRA^-$)] subjects. Wilcoxon paired t-test was used to determine significant differences pre and post vaccination. $P < 0.05$ was considered significant.

Figure 4: Longitudinal analysis reveals that BCG revaccination significantly enhances Ag85A- and BCG-specific IFN-γ and/or IL-2 CD8 T-cell in whole blood. Left hand panel shows ICS data for Ag85A and right-hand panel for BCG following *in vitro* stimulation of whole blood from BCG revaccinated and control subjects. Representative flow cytometry plots show IFN-γ and/or IL-2 cytokine positive $CD8^+$ T-cells after *in vitro* stimulation with either Ag85A (A) or BCG (E) at T0, T2 (A) and T5 (E). Total frequencies of Ag85A (B) and BCG-specific (F) IFN-γ and/or

IL-2 cytokine positive $CD8^+$ T-cells in all participants are shown after background subtraction. Line graphs show changes in frequencies of specific $CD8^+$ T-cells over time in BCG revaccinated [Group 1 ($IGRA^+$, red, N = 19) and Group 2 ($IGRA^-$, blue, N = 18)] subjects and unvaccinated controls [Group 3 ($IGRA^+$, black, N = 18) and Group 4 ($IGRA^-$, brown, N = 18)]. *P* values for longitudinal samples were calculated by comparing each time point to baseline using the Freidman test and corrected for multiple comparisons using Dunn's test. Further, significant differences were determined using the Wilcoxon paired t-test pre and post vaccination. Bonferroni adjusted *P* value threshold of 0.02 was considered statistically significant. Median frequencies of Ag85A (C) and BCG (G) specific IFN-γ and/or IL-2 cytokine-positive $CD8^+$ T-cells over time were compared between unvaccinated and revaccinated $IGRA^+$ and $IGRA^-$ subjects (Group 1 'vs' Group 3 and Group 2 'vs' Group 4). Mann-Whitney *U* test was used to determine significant differences between groups. $P < 0.05$ was considered significant. Analysis of CD45RA and CD27 expression was used to determine percentage distribution of naïve ($CD45RA^+CD27^+$,), central memory (CM, $CD45RA^-CD27^+$), effector memory (EM, $CD45RA^-CD27^-$) and terminally-differentiated T effector memory cells (TD, $CD45RA^+CD27^-$) Ag85A (D) and BCG (H)-specific IFN-γ and/or IL-2 $CD8^+$ T-cells in BCG-revaccinated [Group 1 ($IGRA^+$) and Group 2 ($IGRA^-$)] subjects. Wilcoxon paired t-test was used to determine significant differences pre and post vaccination. $P < 0.05$ was considered significant.

Figure 5: Comparative analysis of whole blood and PBMC ICS assay reveals similar pattern of increase in $CD4^+$ T-cell responses post BCG revaccination. (A) IFN-γ and/or IL-2 frequencies in response to Ag85A (T2) and BCG (T5) stimulation were compared in matched whole blood and PBMC samples from $IGRA^+$ Group 1 subjects. Spearman's correlation coefficient (r) and significance values (P) are indicated. (B) Box and whiskers plots show changes in IFN-γ and/or IL-2

frequencies of $CD4^+$ T-cells over time in BCG revaccinated $IGRA^+$ (Group 1) to *in vitro* Ag85A (left panel) or BCG (right panel) re-stimulation in whole blood (N=19) and PBMC (N=10). Significant differences pre and post-vaccination were determined using the Wilcoxon paired t-test. $P < 0.05$ was considered significant.

Figure 6: COMPASS analysis reveals enhanced polyfunctionality scores in $CD4^+$ and $CD8^+$ T-cell responses in whole blood to Ag85A and BCG stimulation following BCG revaccination. (Compass polyfunctionality scores (PFS) for CD4 and CD8 T-cell subsets were determined for each group and for each antigen stimulation at T0 (baseline), T2 (4 weeks), T4 (10 weeks) and T5 (34 weeks) post-BCG revaccination. Pairwise differences between time points were based on a group wise linear model fit to the PFS (null: βˆ_(T2/T5)-βˆ_T0=0 two-sided test). Polyfunctionality scores were calculated for (Group 1 N=21, Group 2 N=20, Group 3 N=18, Group 4 N=18). Statistical analysis was performed using paired Wilcoxon test compared to baseline.

Figure 7: **COMPASS heat maps showing different polyfunctional $CD4^+$ and $CD8^+$ T-cell subsets post BCG vaccination.** Stacked COMPASS heat maps displaying $CD4^+$ (upper panel) and $CD8^+$ (lower panel) whole blood T-cell responses to Ag85A (left panel) and BCG (right panel) in BCG re-vaccinees [Group 1 ($IGRA^+$, orange) and Group 2 ($IGRA^-$, bright green)] versus unvaccinated controls [Group 3 ($IGRA^+$, light green) and Group 4 ($IGRA^-$,blue)]. In the heat map, columns correspond to the different disjoinT-cell subsets in which responses were detected and are color-coded in the x-axis legend by the cytokines they express (white = “off”, shaded = “on”, grouped by colour = “degree of functionality”), and are displayed in order of increasing functionality from left to right (sky blue to peach). For example, the first

column represents $CD4^+$ T-cells that produce IFN-γ but none of the other functions. Rows represent study subjects (Group 1 N=21, Group 2 N=20, Group 3 N=18, Group 4 N=18), which are ordered by the group they belong to and the time point [0 (turquoise) and 4 (pink) weeks for Ag85A and 0 (turquoise) and 34 (pink) weeks for BCG] as shown in the legend at the right. Each cell of the heatmap shows the probability estimated by COMPASS that the observed response is antigen-specific in the corresponding subject (row) and cell subset (column), where the probability is color-coded from white (zero) to purple (one). A probability of 0 indicates certainty that the observed response is background, while a probability of 1 indicates certainty that the observed response is antigen-specific. Horizontal lines were added to separate the time points and red boxes were inserted to highlight the subsets of interest.

Figure 8: Polyfunctional $CD4^+$ T-cell responses induced upon BCG revaccination are comparable in whole blood and PBMC of BCG revaccinated $IGRA^+$ subjects. (A) Polyfunctionality scores at T5 were calculated for $CD4^+$ T-cells post re-stimulation of whole blood (Group 1 N=21, Group 2 N=20, Group 3 N=18, Group 4 N=18) with Ag85A or BCG taking into account T-cells positive for IL-2, IFN-γ, TNF-α, IL-17A and MIP-1β. (B) Similarly, polyfunctionality scores at T5 were calculated for $CD4^+$ T-cells post re-stimulation of PBMCs (N=10) with Ag85A, BCG or LTAg taking into account T-cells positive for IFN-γ, IL-2, TNFα, IL-17A, IL-17F, IL-22, IL-10 and MIP-1β. Box and whisker plots show comparison of COMPASS polyfunctionality scores (PFS) between revaccinated subjects (Group 1 & 2) and unvaccinated subjects (Group 3 & 4) in both whole blood and PBMCs. Statistical significance of differences between groups was determined by Mann-Whitney *U* test. $P < 0.05$ was considered significant.

Figure 9: BCG revaccination significantly induces Mtb-specific cytokines in PBMC. Representative flow cytometry plots (upper panel) show total IFN-γ, IL-17A, IL-17F, IL-22 and IL-10 cytokine positive $CD4^+$ T-cells after *in vitro* stimulation with BCG at T5 in Group 1 vs Group 3 subject. The flow cytometry plots for the same donors from Group 1 and 3 for BCG stimulation are shown again in Supplemental Figure 4 and 5. Mtb-specific T-cell responses in PBMCs from BCG revaccinated $IGRA^+$ and $IGRA^-$ subjects (Group 1 & 2, N=10) were compared with unvaccinated control $IGRA^+$ and $IGRA^-$ subjects (Group 3 & 4, N=10) in a standard ICS assay (lower panel). PBMCs were stimulated with Ag85A or BCG or a pool of LTAg (Rv1733c, Rv1737c, Rv2029 & Rv2628). $CD3^+CD4^+$ T-cells were analysed for intracellular expression of indicated cytokines. Scatter plots show median (range) percentages of total IFN-γ, IL-17A, IL-17F, IL-22 and IL-10-positive $CD4^+$ T-cells. Unadjusted p-values were calculated with the Mann-Whitney U-test, comparing frequencies of cytokine-positive cells between the two groups. To correct for multiple testing (Bonferroni method), P-values below 0.025 were considered statistically significant.

Figure 10: BCG revaccination significantly induces Mtb-specific regulatory IL-10^+Th17 responses. $CD4^+$ T-cell subsets expressing IL-17A, IL-17F, or IL-22 (Th17) either in combination with IFN-γ or IL-10 from BCG revaccinated $IGRA^+$ and $IGRA^-$ subjects (Group 1 & 2, N=10) were compared with unvaccinated control $IGRA^+$ and $IGRA^-$ subjects (Group 3 & 4, N=10) at T5 post-BCG vaccination to Ag85A, BCG and LTAg stimulation. For this analysis, we calculated cytokine-positive cells based on the gating shown in Supplemental Figure 6. Statistical analysis was performed using a one-way ANOVA with Bonferroni post hoc test defining differences as significant ($*p < 0.05$).

Figure 11: BCG revaccination induces innate effector response in whole blood. Line graphs show the frequencies of IFN-γ-expressing γδ T, NKT, $CD56^{br}$ NK and $CD56^{dim}$ NK cells in BCG revaccinated $IGRA^+$ and $IGRA^-$ subjects (Group 1, N=20 & Group 2, N=18) versus unvaccinated control $IGRA^+$ and $IGRA^-$ subjects (Group 3, N=19 & Group 4, N=18) to Ag85A and BCG stimulation at baseline and at T2 and T5 post-BCG revaccination respectively. Significance between longitudinal samples in a group was calculated using Wilcoxon matched pairs test. $P<0.05$ was considered significant.

Table 1: Clinical Characteristics of Study Recruits. Median age for all the clinical group is 20 or close to 20 except group 3 is 19. Male-female ratio in each clinical group is close to 1 except group 4. There was no significance difference found between male-female IGRA level (QuantiFERON-TB Gold) except group 1 (P=0.01), however there was no significance difference between male-female background $CD4^+$ IFN-γ and/or IL-2 expression stimulated with Ag85A or BCG.

GROUP	N	Median Age (Range)	Male (%)	Female (%)	IGRA level median (Range)
1	21	20 (19-28)	42.86	57.14	3.6 (0.46-10)
2	23	20 (18-23)	39.1	60.87	0.04 (0.01-0.3)
3	18	19 (18-23)	61.11	38.89	2 (0.58-10)
4	18	19.5 (18-23)	22.22	77.78	0.1 (0-0.3)

SUPPLEMENTAL FIGURE LEGENDS

Supplemental Figure 1: Flow cytometry gating strategy for T-cell analysis in whole blood. Schematic representation of flow cytometry plots showing sequential gating strategy of whole blood cells for analysis of $CD4^+$ and $CD8^+$ T-cells. All gates for non-functional markers were defined using fluorescence minus one (FMO) controls; gates for functional markers were defined using the unstimulated samples. Initial gating was done on FSC-H and FSC-A to discriminate singlets, followed by the exclusion of $CD14^+$ monocytes. Lymphocytes were gated using FSC-A and SSC-A. Within the lymphocyte gate, $CD3^+$ cells were identified, followed by $CD4^+$ and $CD8^+$ T-cells. CD27 and CD45RA expression within $CD4^+$ and $CD8^+$ T-cell subsets was used to define memory phenotypes (naïve, CM, EM and TD). To define functional markers for $CD4^+$ and $CD8^+$ T-cells, a gate was applied for each cytokine, not taking into account the co-expression of other markers. Boolean gates were then created based on these gates to identify cells expressing different combinations of markers.

Supplemental Figure 2: TB10.4-specific $CD4^+$ and $CD8^+$ T-cell responses in whole blood before and after BCG revaccination. Line graphs show changes in TB10.4 specific IFN-γ and/or IL-2 frequencies of $CD4^+$ and $CD8^+$ T-cells over time in BCG vaccinated $IGRA^+$ (Group 1, N=19) and $IGRA^-$ (Group 2, N=18) subjects versus unvaccinated control $IGRA^+$ (Group 3, N=18) and $IGRA^-$ (Group 4, N=18) subjects.

Supplemental Figure 3: Flow cytometry gating strategy for T-cell analysis in PBMC. Schematic representation of flow cytometry plots showing sequential gating strategy of PBMCs for analysis of $CD4^+$ and $CD8^+$ T-cells. All gates for non-functional markers were defined using fluorescence minus one (FMO) controls; gates for functional markers were defined using the unstimulated samples. Initial gating was done on FSC-H and FSC-A to discriminate singlets, followed by the exclusion of dead cells by AVID stain. Lymphocytes were gated using FSC-A and SSC-A. Within the lymphocyte gate, $CD3^+$ cells were identified, followed by $CD4^+$ and $CD8^+$ T-cells.

To define functional markers for $CD4^+$ T-cells, a gate was applied for each cytokine, not taking into account the co-expression of other markers. Boolean gates were then created based on these gates to identify cells expressing different combinations of markers.

Supplemental Figure 4: $CD4^+$ T-cell cytokine responses in PBMC to BCG stimulation. Representative flow cytometry plots (from same donors as shown in Figure 9) show total IFN-γ, IL-2, IL-17A, IL-17F, IL-22 and IL-10 cytokine positive $CD4^+$ T-cells in unstimulated control and after *in vitro* stimulation with BCG at T5 in Group 1 versus Group 3 subjects.

Supplemental Figure 5: Th17 subsets in PBMC to Mtb antigens and BCG stimulation. Representative flow cytometry plots (from same donors as shown in Figure 9) show $CD4^+$Th17 subsets expressing either IFN-γ or IL-10 with IL-17F with or without *in vitro* stimulation of PBMC with Ag85A, BCG, LTAg at T5 in a Group 1 subject. The quadrant gates for the cytokines were positioned closer to the negative cells for these analyses to examine the Th17 double-positive cells. Since those cells are rare and the MFI of the cytokines on those cells is low, the lower position of the quadrant was necessary to include those cells.

Supplemental Figure 6: Th17 subsets in PBMC to BCG stimulation. Representative flow cytometry plots show $CD4^+$Th17 subsets expressing either IFN-γ or IL-10 with IL-17F with or without *in vitro* stimulation of PBMC with BCG at T5 in two additional Group 1 subjects.

Supplemental Figure 7: Gating Strategy for Innate Cells. A representative sequential gating strategy for NKT, $CD56^{br}$ NK, $CD56^{dim}$ NK and $\gamma\delta$ T-cells in whole blood is shown. Frequencies of IFN-γ expressing cells were studied in all populations.

Supplemental Figure 8: BCG revaccination did not impact Hep B antibody titer in study participants. Hep B antibody titer was measured in plasma of study participants at T0, T1, T2, T4 and T5. Antibody titer was measured by standard ELISA and concentration was expressed as IU/ml. N for Group 1 = 16, Group 2=10, Group 3=16 and Group 4=10. P values for longitudinal samples were calculated by comparing each time point to baseline using the Freidman test and corrected for multiple comparisons using Dunn's test.

Supplemental Table 1: Panel of antibodies used for cell surface and intracellular markers for (A) whole blood and (B) PBMC ICS assays.

Supplemental File 1: Clinical details of study participants who were included in final data analysis.

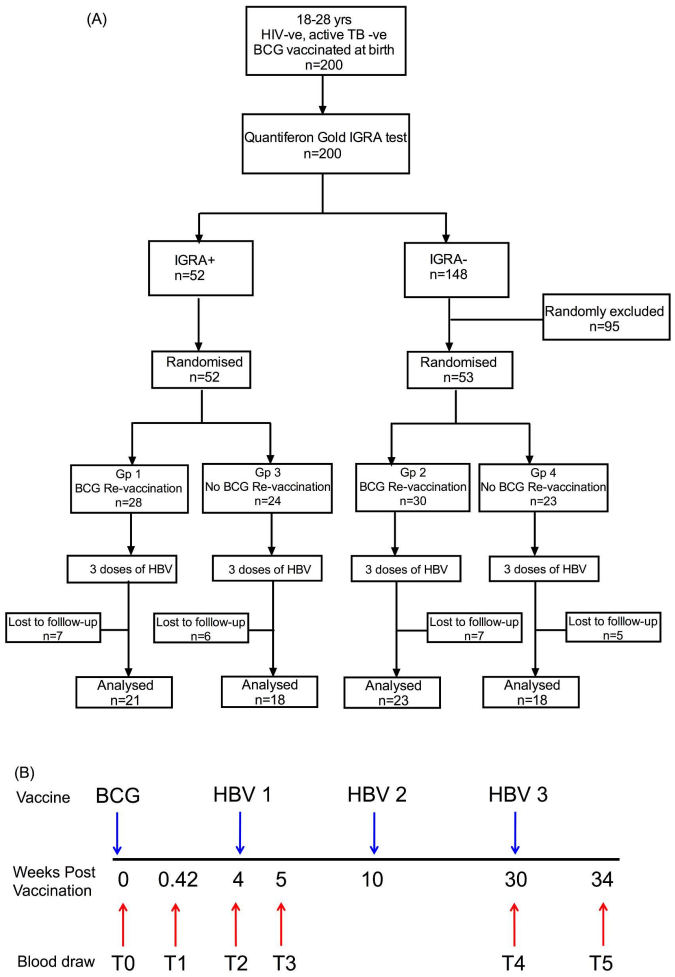

Figure 1: Overall study design. (A) CONSORT flow diagram of participant recruitment and enrolment. (B) A diagrammatic representation of study design including schedule of vaccination and blood draw. Group 1 and Group 2 received BCG at day 0 (T0) and then three doses of HBV vaccine at weeks 4 (T2), 10 and 30 (T4). Group 3 and Group 4 did not receive BCG vaccine but three doses of HBV. Immunization time points are shown by blue arrows and the six blood sampling time points (T0-T5) are indicated by red arrows for all groups.

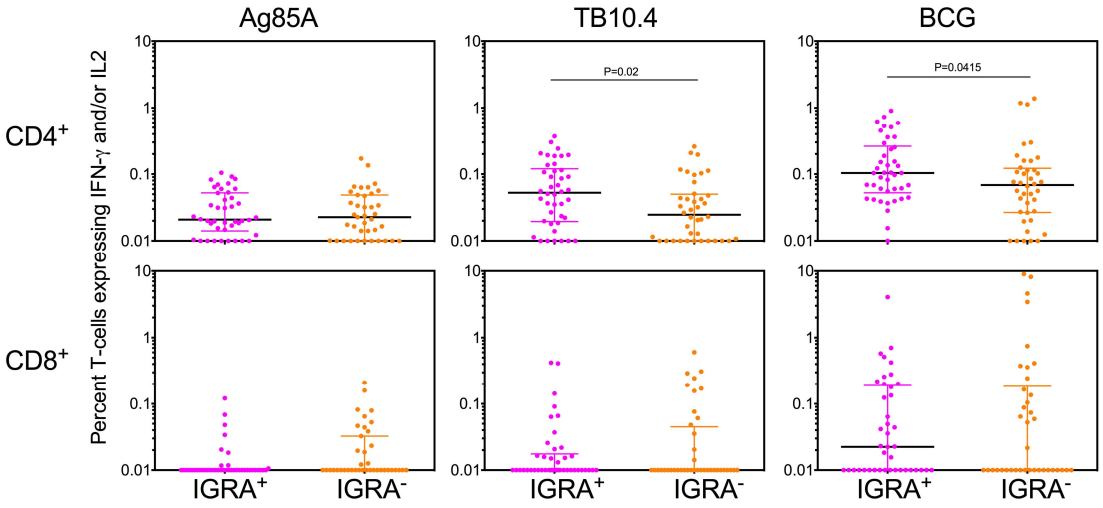

Figure 2: Baseline Mtb antigen-specific T-cell responses in whole blood of IGRA$^+$ vs. IGRA$^-$ subjects. Scatter plots of Ag85A, TB10.4 and BCG reactive IFN-γ and/or IL-2 expressing CD4$^+$ (upper panels) and CD8$^+$ (lower panels) T-cells in whole blood are shown after background subtraction at baseline in IGRA$^+$ vs. IGRA$^-$ subjects. Number of subjects in each group range from 38 to 42. Significant differences between groups were determined using the Mann–Whitney U test (*P* values < 0.05 are shown).

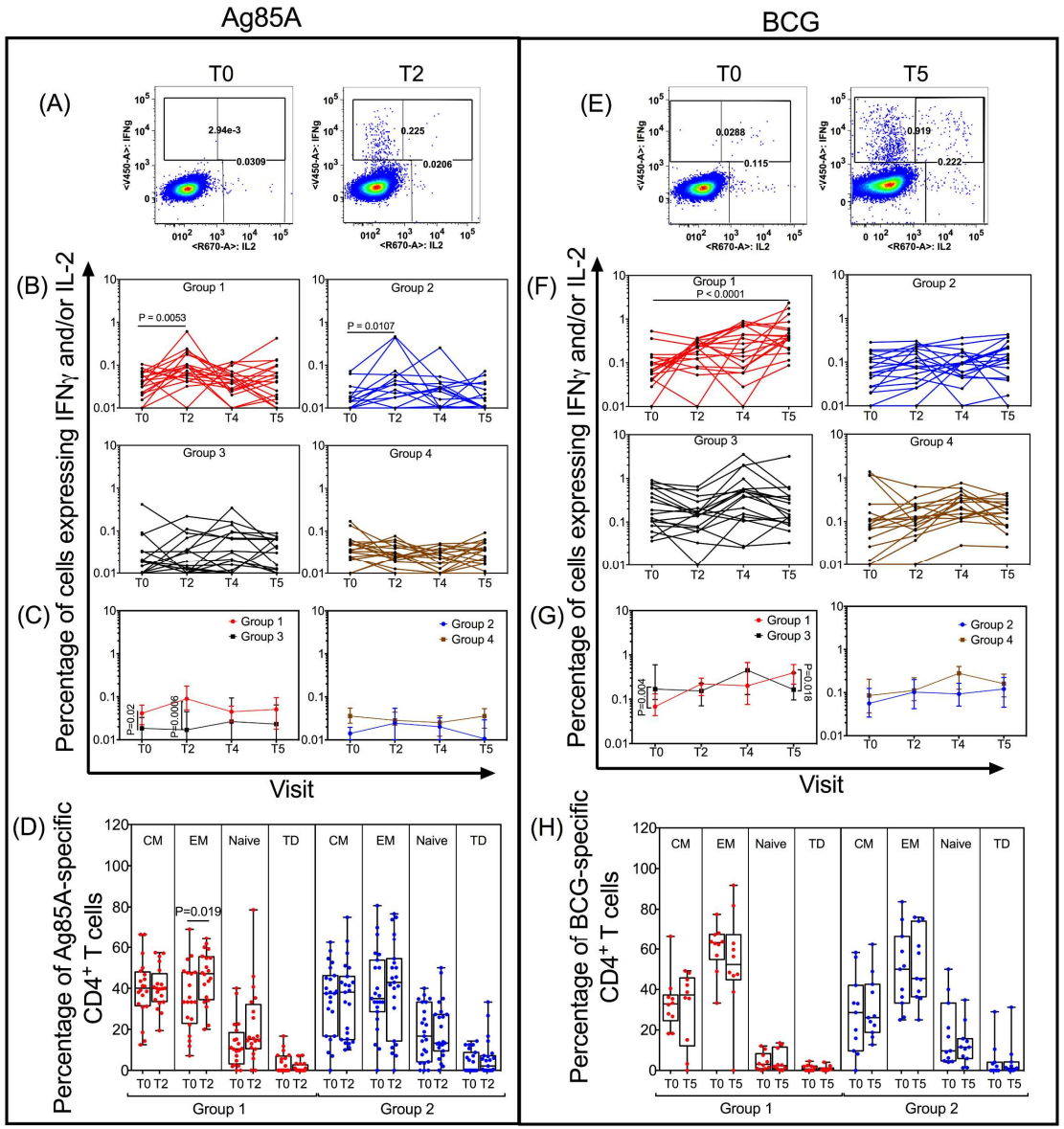

Figure 3: Longitudinal analysis reveals that BCG revaccination significantly enhances Ag85A- and BCG-specific IFN-γ and/or IL-2 CD4 T-cell responses in whole blood. Left hand panel shows ICS data for Ag85A and right-hand panel for BCG following *in vitro* stimulation of whole blood from BCG revaccinated and control subjects. Representative flow cytometry plots show IFN-γ and/or IL-2 cytokine positive $CD4^+$ T-cells after *in vitro* stimulation with either Ag85A (A) or BCG (E) at T0, T2 (A) and T5 (E). Total frequencies of Ag85A (B) and BCG-specific (F) IFN-γ and/or IL-2 cytokine-positive $CD4^+$ T-cells in all participants are shown after background subtraction. Line graphs show changes in frequencies of specific $CD4^+$ T-cells over time in BCG revaccinated [Group 1 ($IGRA^+$, red, N = 19) and Group 2 ($IGRA^-$, blue, N = 18)] subjects and unvaccinated controls [Group 3 ($IGRA^+$, black, N = 18) and Group 4 ($IGRA^-$, brown, N = 18)]. P values for longitudinal samples were calculated by comparing each time point to baseline using the Freidman test and corrected for multiple comparisons using Dunn's test. Further, significant differences were determined using the Wilcoxon paired t-test pre and post vaccination. Bonferroni adjusted *P* value threshold of 0.02 was considered statistically significant. Median frequencies of Ag85A (C) and BCG (G) specific IFN-γ and/or IL-2 cytokine positive $CD4^+$ T-cells over time were compared between unvaccinated and revaccinated $IGRA^+$ and $IGRA^-$ subjects (Group 1 vs Group 3 and Group 2 vs Group 4). Mann-Whitney *U* test was used to determine significant differences between groups. $P < 0.05$ was considered significant. Analysis of CD45RA and CD27 expression was used to determine percentage distribution of naïve ($CD45RA^+CD27^+$,), central memory (CM, $CD45RA^-CD27^+$), effector memory (EM, $CD45RA^-CD27^-$) and terminally-differentiated T effector memory cells (TD, $CD45RA^+CD27^-$) Ag85A (D) and BCG (H)-specific IFN-γ and/or IL-2 $CD4^+$ T-cells in BCG-revaccinated [Group 1 ($IGRA^+$) and Group 2 ($IGRA^-$)] subjects. Wilcoxon paired t-test was used to determine significant differences pre and post vaccination. $P < 0.05$ was considered significant.

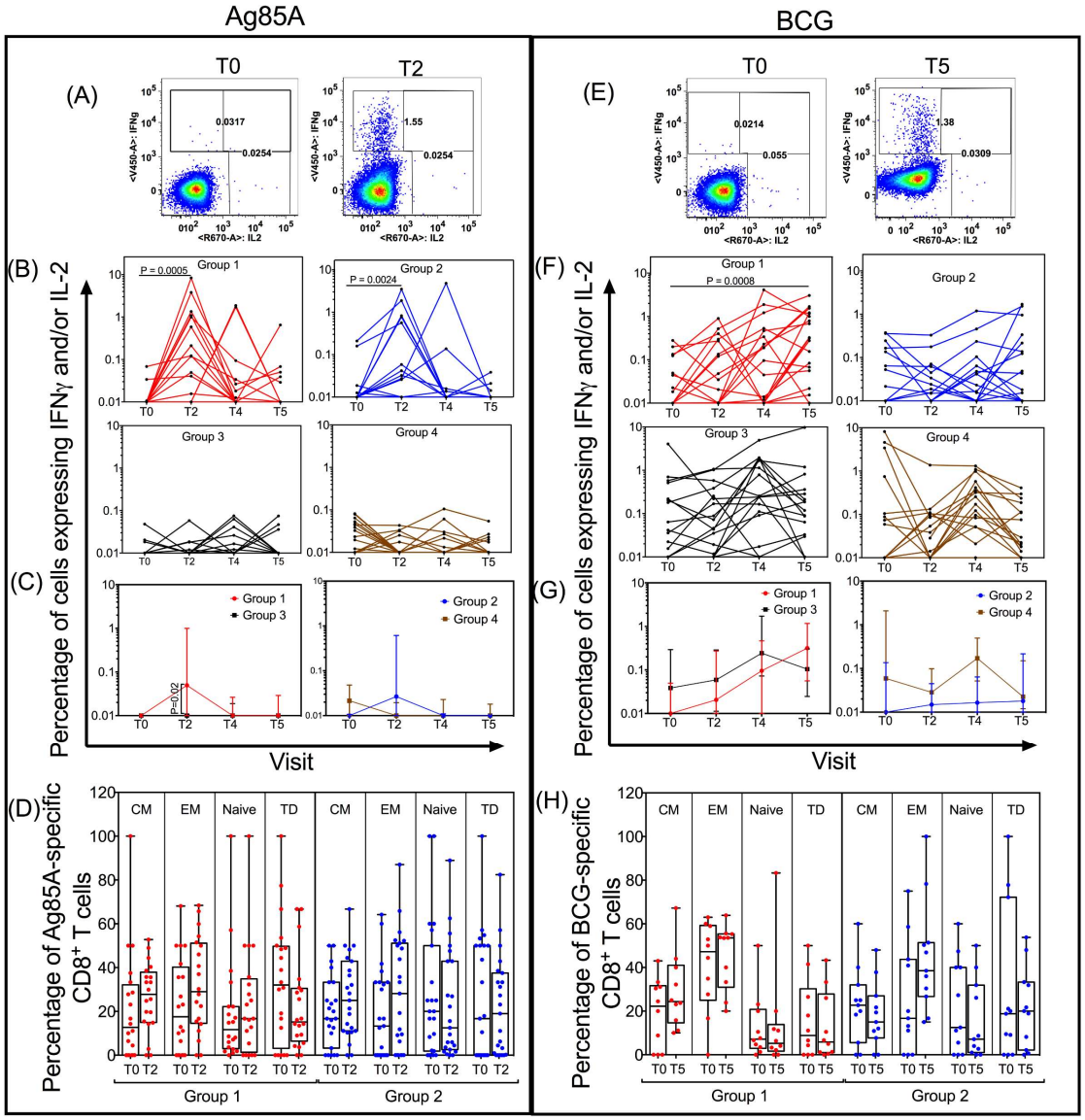

Figure 4: Longitudinal analysis reveals that BCG revaccination significantly enhances Ag85A- and BCG-specific IFN-γ and/or IL-2 CD8 T-cell in whole blood. Left hand panel shows ICS data for Ag85A and right-hand panel for BCG following *in vitro* stimulation of whole blood from BCG revaccinated and control subjects. Representative flow cytometry plots show IFN-γ and/or IL-2 cytokine positive $CD8^+$ T-cells after *in vitro* stimulation with either Ag85A (A) or BCG (E) at T0, T2 (A) and T5 (E). Total frequencies of Ag85A (B) and BCG-specific (F) IFN-γ and/or IL-2 cytokine positive $CD8^+$ T-cells in all participants are shown after background subtraction. Line graphs show changes in frequencies of specific $CD8^+$ T-cells over time in BCG revaccinated [Group 1 ($IGRA^+$, red, N = 19) and Group 2 ($IGRA^-$, blue, N = 18)] subjects and unvaccinated controls [Group 3 ($IGRA^+$, black, N = 18) and Group 4 ($IGRA^-$, brown, N = 18)]. *P* values for longitudinal samples were calculated by comparing each time point to baseline using the Freidman test and corrected for multiple comparisons using Dunn's test. Further, significant differences were determined using the Wilcoxon paired t-test pre and post vaccination. Bonferroni adjusted *P* value threshold of 0.02 was considered statistically significant. Median frequencies of Ag85A (C) and BCG (G) specific IFN-γ and/or IL-2 cytokine-positive $CD8^+$ T-cells over time were compared between unvaccinated and revaccinated $IGRA^+$ and $IGRA^-$ subjects (Group 1 'vs' Group 3 and Group 2 'vs' Group 4). Mann-Whitney *U* test was used to determine significant differences between groups. $P < 0.05$ was considered significant. Analysis of CD45RA and CD27 expression was used to determine percentage distribution of naïve ($CD45RA^+CD27^+$,), central memory (CM, $CD45RA^-CD27^+$), effector memory (EM, $CD45RA^-CD27^-$) and terminally-differentiated T effector memory cells (TD, $CD45RA^+CD27^-$) Ag85A (D) and BCG (H)-specific IFN-γ and/or IL-2 $CD8^+$ T-cells in BCG-revaccinated [Group 1 ($IGRA^+$) and Group 2 ($IGRA^-$)] subjects. Wilcoxon paired t-test was used to determine significant differences pre and post vaccination. $P < 0.05$ was considered significant.

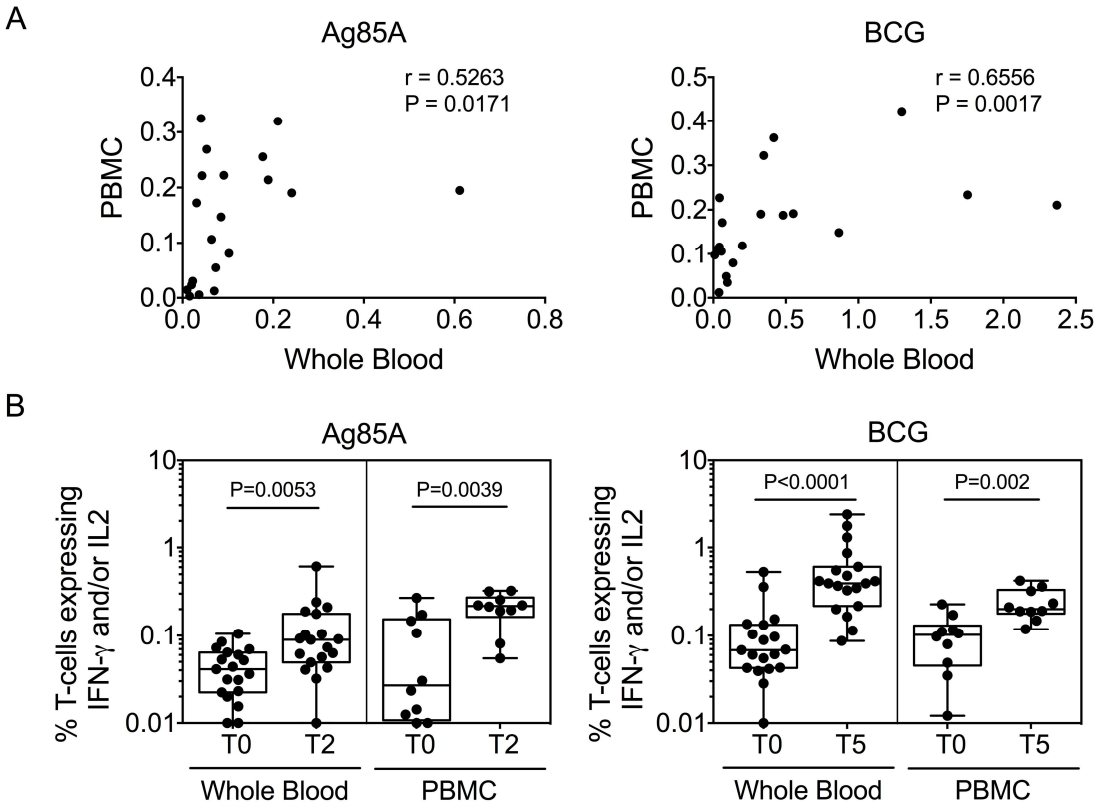

Figure 5: Comparative analysis of whole blood and PBMC ICS assay reveals similar pattern of increase in CD4⁺ T-cell responses post BCG revaccination. (A) IFN-γ and/or IL-2 frequencies in response to Ag85A (T2) and BCG (T5) stimulation were compared in matched whole blood and PBMC samples from IGRA⁺ Group 1 subjects. Spearman's correlation coefficient (r) and significance values (P) are indicated. (B) Box and whiskers plots show changes in IFN-γ and/or IL-2 frequencies of CD4⁺ T-cells over time in BCG revaccinated IGRA⁺ (Group 1) to *in vitro* Ag85A (left panel) or BCG (right panel) re-stimulation in whole blood (N=19) and PBMC (N=10). Significant differences pre and post-vaccination were determined using the Wilcoxon paired t-test. $P < 0.05$ was considered significant.

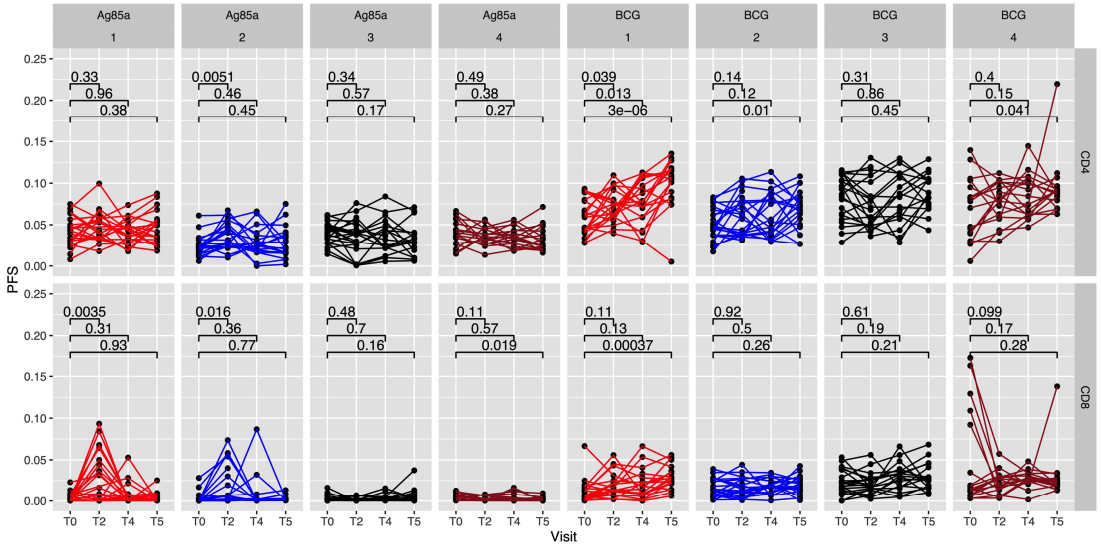

Figure 6: COMPASS analysis reveals enhanced polyfunctionality scores in CD4⁺ and CD8⁺ T-cell responses in whole blood to Ag85A and BCG stimulation following BCG revaccination. (Compass polyfunctionality scores (PFS) for CD4 and CD8 T-cell subsets were determined for each group and for each antigen stimulation at T0 (baseline), T2 (4 weeks), T4 (10 weeks) and T5 (34 weeks) post-BCG revaccination. Pairwise differences between time points were based on a group wise linear model fit to the PFS (null: βˆ_(T2/T5)-βˆ_T0=0 two-sided test). Polyfunctionality scores were calculated for (Group 1 N=21, Group 2 N=20, Group 3 N=18, Group 4 N=18). Statistical analysis was performed using paired Wilcoxon test compared to baseline.

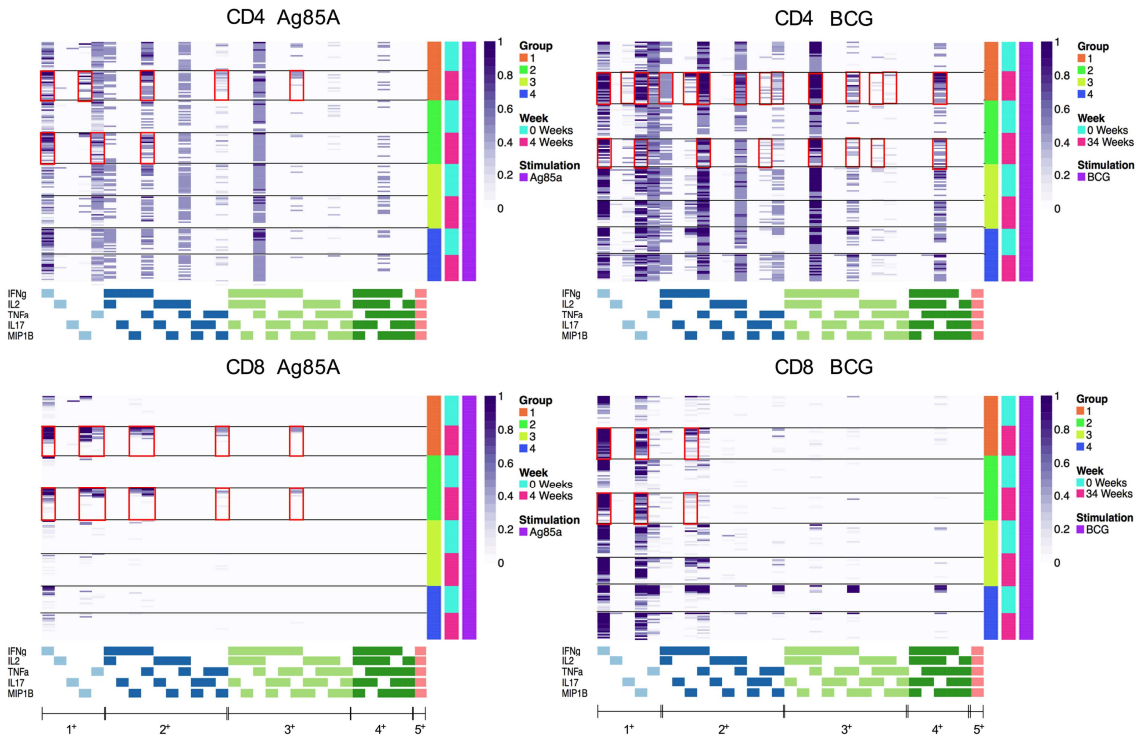

Figure 7: **COMPASS heat maps showing different polyfunctional CD4⁺ and CD8⁺ T-cell subsets post BCG vaccination.** Stacked COMPASS heat maps displaying CD4⁺ (upper panel) and CD8⁺ (lower panel) whole blood T-cell responses to Ag85A (left panel) and BCG (right panel) in BCG re-vaccinees [Group 1 (IGRA⁺, orange) and Group 2 (IGRA⁻, bright green)] versus unvaccinated controls [Group 3 (IGRA⁺, light green) and Group 4 (IGRA⁻,blue)]. In the heat map, columns correspond to the different T-cell subsets in which responses were detected and are color-coded in the x-axis legend by the cytokines they express (white = "off", shaded = "on", grouped by colour = "degree of functionality"), and are displayed in order of increasing functionality from left to right (sky blue to peach). For example, the first column represents CD4⁺ T-cells that produce IFN-γ but none of the other functions. Rows represent study subjects (Group 1 N=21, Group 2 N=20, Group 3 N=18, Group 4 N=18), which are ordered by the group they belong to and the time point [0 (turquoise) and 4 (pink) weeks for Ag85A and 0 (turquoise) and 34 (pink) weeks for BCG] as shown in the legend at the right. Each cell of the heatmap shows the probability estimated by COMPASS that the observed response is antigen-specific in the corresponding subject (row) and cell subset (column), where the probability is color-coded from white (zero) to purple (one). A probability of 0 indicates certainty that the observed response is background, while a probability of 1 indicates certainty that the observed response is antigen-specific. Horizontal lines were added to separate the time points and red boxes were inserted to highlight the subsets of interest.

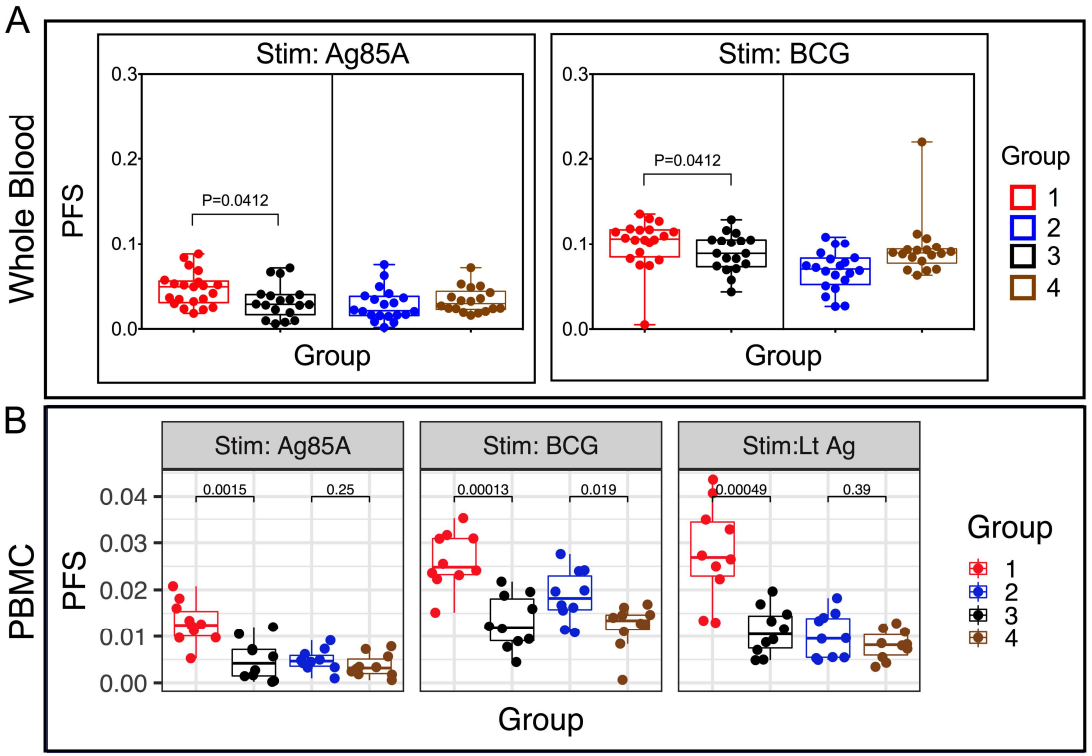

Figure 8: Polyfunctional CD4⁺ T-cell responses induced upon BCG revaccination are comparable in whole blood and PBMC of BCG revaccinated IGRA⁺ subjects. (A) Polyfunctionality scores at T5 were calculated for CD4⁺ T-cells post re-stimulation of whole blood (Group 1 N=21, Group 2 N=20, Group 3 N=18, Group 4 N=18) with Ag85A or BCG taking into account T-cells positive for IL-2, IFN-γ, TNF-α, IL-17A and MIP-1β. (B) Similarly, polyfunctionality scores at T5 were calculated for CD4⁺ T-cells post re-stimulation of PBMCs (N=10) with Ag85A, BCG or LTAg taking into account T-cells positive for IFN-γ, IL-2, TNFα, IL-17A, IL-17F, IL-22, IL-10 and MIP-1β. Box and whisker plots show comparison of COMPASS polyfunctionality scores (PFS) between revaccinated subjects (Group 1 & 2) and unvaccinated subjects (Group 3 & 4) in both whole blood and PBMCs. Statistical significance of differences between groups was determined by Mann-Whitney *U* test. $P < 0.05$ was considered significant.

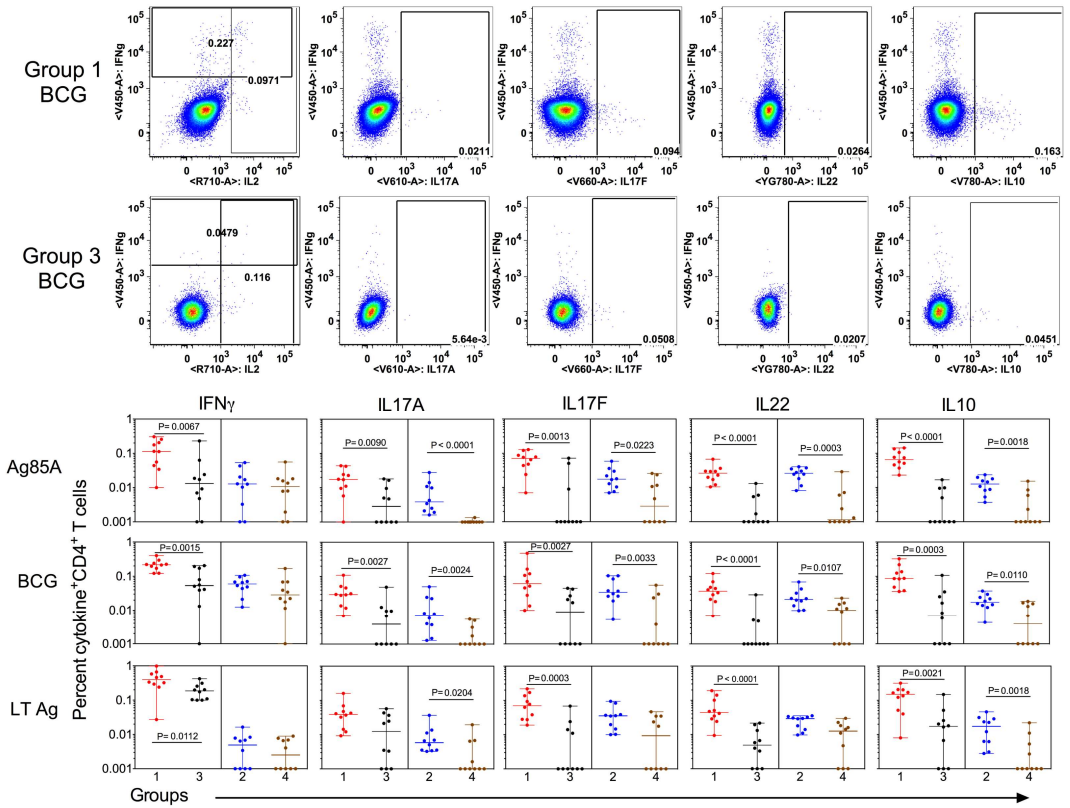

Figure 9: BCG revaccination significantly induces Mtb-specific cytokines in PBMC. Representative flow cytometry plots (upper panel) show total IFN-γ, IL-17A, IL-17F, IL-22 and IL-10 cytokine positive CD4⁺ T-cells after *in vitro* stimulation with BCG at T5 in Group 1 vs Group 3 subject. The flow cytometry plots for the same donors from Group 1 and 3 for BCG stimulation are shown again in Supplemental Figure 4 and 5. Mtb-specific T-cell responses in PBMCs from BCG revaccinated IGRA⁺ and IGRA⁻ subjects (Group 1 & 2, N=10) were compared with unvaccinated control IGRA⁺ and IGRA⁻ subjects (Group 3 & 4, N=10) in a standard ICS assay (lower panel). PBMCs were stimulated with Ag85A or BCG or a pool of LTAg (Rv1733c, Rv1737c, Rv2029 & Rv2628). $CD3^+CD4^+$ T-cells were analysed for intracellular expression of indicated cytokines. Scatter plots show median (range) percentages of total IFN-γ, IL-17A, IL-17F, IL-22 and IL-10-positive CD4⁺ T-cells. Unadjusted p-values were calculated with the Mann-Whitney U-test, comparing frequencies of cytokine-positive cells between the two groups. To correct for multiple testing (Bonferroni method), P-values below 0.025 were considered statistically significant.

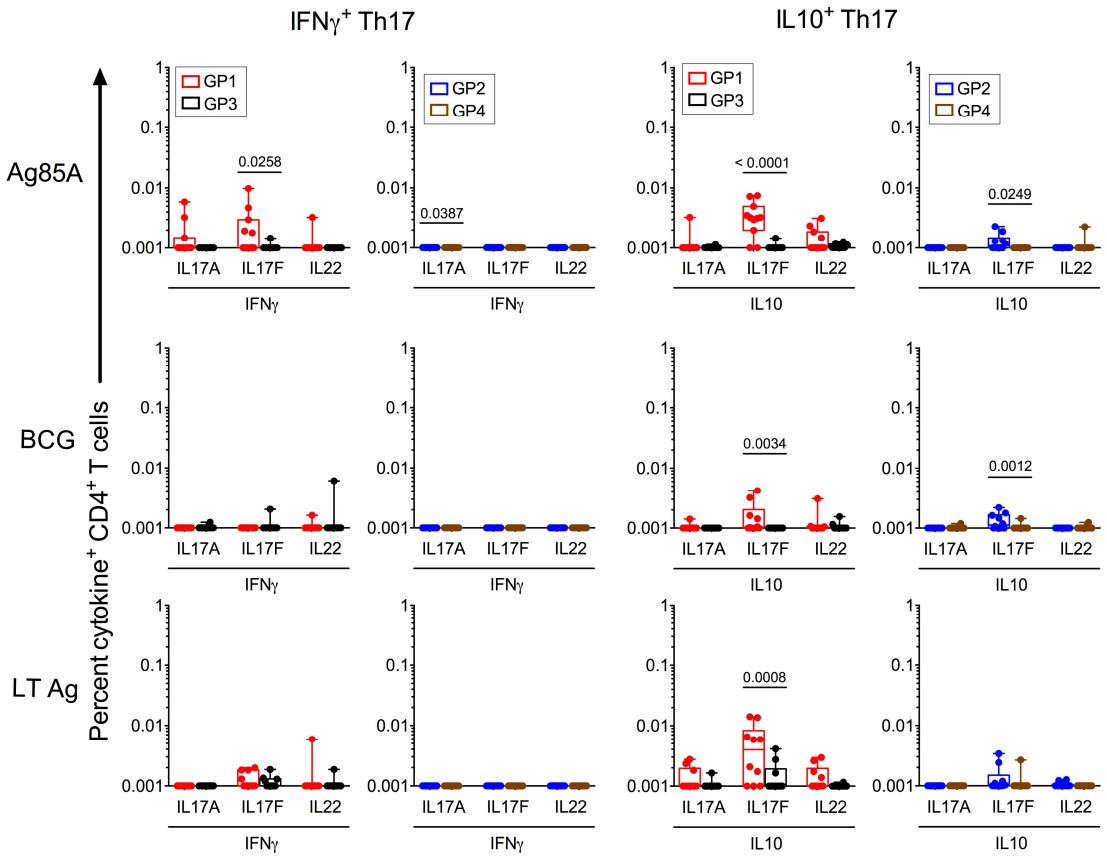

Figure 10: BCG revaccination significantly induces Mtb-specific regulatory IL-10⁺Th17 responses. CD4⁺ T-cell subsets expressing IL-17A, IL-17F, or IL-22 (Th17) either in combination with IFN-γ or IL-10 from BCG revaccinated IGRA⁺ and IGRA⁻ subjects (Group 1 & 2, N=10) were compared with unvaccinated control IGRA⁺ and IGRA⁻ subjects (Group 3 & 4, N=10) at T5 post-BCG vaccination to Ag85A, BCG and LTAg stimulation. For this analysis, we calculated cytokine-positive cells based on the gating shown in Supplemental Figure 6. Statistical analysis was performed using a one-way ANOVA with Bonferroni post hoc test defining differences as significant (*$p < 0.05$).

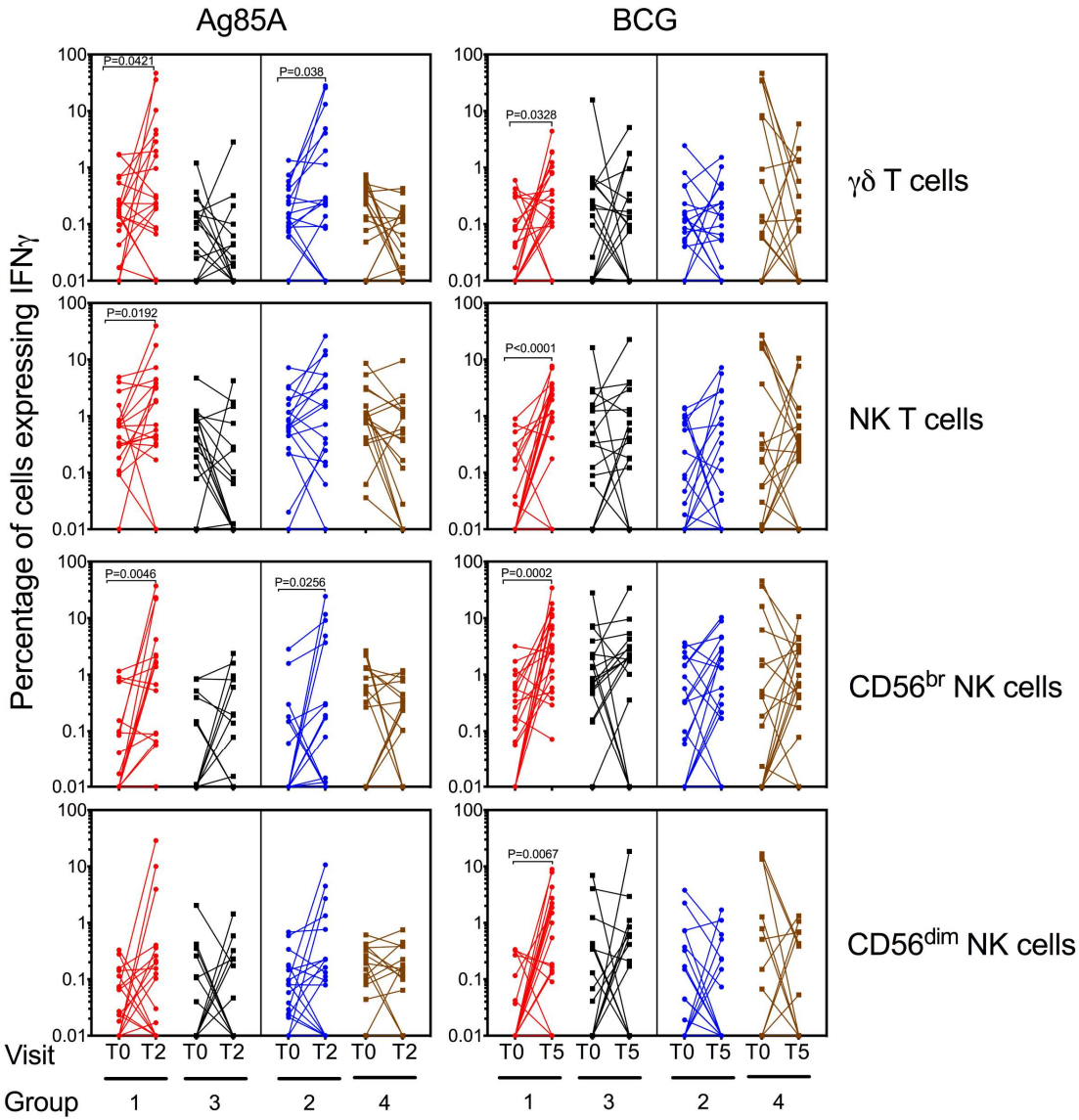

Figure 11: BCG revaccination induces innate effector response in whole blood. Line graphs show the frequencies of IFN-γ-expressing γδ T, NKT, $CD56^{br}$ NK and $CD56^{dim}$ NK cells in BCG revaccinated $IGRA^+$ and $IGRA^-$ subjects (Group 1, N=20 & Group 2, N=18) versus unvaccinated control $IGRA^+$ and $IGRA^-$ subjects (Group 3, N=19 & Group 4, N=18) to Ag85A and BCG stimulation at baseline and at T2 and T5 post-BCG revaccination respectively. Significance between longitudinal samples in a group was calculated using Wilcoxon matched pairs test. P<0.05 was considered significant.